



HAL
open science

New age constraints on the timing of volcanism in central Afar, in the presence of propagating rifts

Pierre Lahitte, Pierre-Yves Gillot, Tesfaye Kidane, Vincent Courtillot, Abebe Bekele

► **To cite this version:**

Pierre Lahitte, Pierre-Yves Gillot, Tesfaye Kidane, Vincent Courtillot, Abebe Bekele. New age constraints on the timing of volcanism in central Afar, in the presence of propagating rifts. *Journal of Geophysical Research: Solid Earth*, 2003, 108, p. 289-310. 10.1029/2001JB001689 . insu-03598426

HAL Id: insu-03598426

<https://insu.hal.science/insu-03598426>

Submitted on 6 Mar 2022

HAL is a multi-disciplinary open access archive for the deposit and dissemination of scientific research documents, whether they are published or not. The documents may come from teaching and research institutions in France or abroad, or from public or private research centers.

L'archive ouverte pluridisciplinaire **HAL**, est destinée au dépôt et à la diffusion de documents scientifiques de niveau recherche, publiés ou non, émanant des établissements d'enseignement et de recherche français ou étrangers, des laboratoires publics ou privés.

Copyright

New age constraints on the timing of volcanism in central Afar, in the presence of propagating rifts

Pierre Lahitte and Pierre-Yves Gillot

Laboratoire de Géochronologie Multi-Techniques UPS-IPGP, Université Paris-Sud, Orsay, France

Tesfaye Kidane¹ and Vincent Courtillot

Laboratoires de Paléomagnétisme et de Tectonique, Institut de Physique du Globe de Paris, Paris, France

Abebe Bekele

Department of Geology and Geophysics, University of Addis-Ababa, Addis-Ababa, Ethiopia

Received 3 December 2001; revised 25 June 2002; accepted 26 August 2002; published 26 February 2003.

[1] We investigate the relationship between rift propagation and volcanism in the Afar Depression in the last 4 Myr. Potassium-argon and thermoluminescence dating allow detailed reconstruction of the temporal evolution of volcanism. Volcanic activity is almost continuous since 3.5 Ma, with intervals characterized by more intense activity, especially around 2 Ma. Spatial distribution of ages reveals that Stratoid Series volcanism migrated northward along a 200-km trend between 3 and 1 Ma, at about 10 cm/yr, linked to northward propagation of the Gulf of Aden Ridge, after it had cut across the Danakil horst at 4 Ma. Our work underlines the role of rhyolitic volcanism in initiation of rifting. Acid volcanoes, initially formed near the axes of extensional zones, have been subsequently dissected and are presently located on both sides of active rift segments. These lavas were the first to be erupted in areas of low extensional strain and were followed by basaltic lavas as extension increased. Differentiated volcanoes acted as zones of local weakness and guided localization of fractures, then leading to fissural magmatism. This regional-scale, composite style of rifting, including volcanic and tectonic components, can be compared to the large-scale continental breakup process itself. Deformation occurs through propagation of faults and fissures under a regional stress field. These become localized because of weakening of the crust (or lithosphere) due to emplacement of magmas, under the influence of a plume in the large-scale case, or of silicic centers linked to magma chambers in the regional-scale case. *INDEX TERMS:* 1035 Geochemistry:

Geochronology; 8109 Tectonophysics: Continental tectonics—extensional (0905); 8150 Tectonophysics: Evolution of the Earth: Plate boundary—general (3040); 8439 Volcanology: Physics and chemistry of magma bodies; *KEYWORDS:* Afar, geochronology, volcanism, rift propagation, Ethiopia, K/Ar dating

Citation: Lahitte, P., P.-Y. Gillot, T. Kidane, V. Courtillot, and A. Bekele, New age constraints on the timing of volcanism in central Afar, in the presence of propagating rifts, *J. Geophys. Res.*, 108(B2), 2123, doi:10.1029/2001JB001689, 2003.

1. Introduction

[2] The Afar Depression (AD) is often considered as a classical example of a triple rift junction. It lies at the intersection of the Gulf of Aden and Red Sea oceanic ridges with the East African continental rift (EAR) (Figure 1a). Its northeastern edge is bounded by the Danakil microplate, while its western and southern borders follow the escarpments of the Ethiopian and Somalian plateaus. Before separation from their Yemen counterpart, they formed a single continental trap (or flood basalt) formation, emplaced

about 30 Ma [Hofmann *et al.*, 1997; Coulié *et al.*, 2000]. The relationship between trap emplacement and the continental breakup is a matter of debate [e.g., Courtillot *et al.*, 1999; King and Anderson, 1995; White and McKenzie, 1989]; the association of the tectonics of the Afar triple junction with the Afar plume has been suggested since Schilling [1973]. The resulting complex regional history can be summarized by a two-phase model in which Arabia-Africa rifting first started along an East African Rift-Red Sea path (30–20 Ma) and then continued along a Gulf of Aden-Red Sea path (20–0 Ma) [Courtillot *et al.*, 1987]. This has led to breakup of the traps into three parts and to the formation of the AD. At present, the Afar floor lies as much as 1500 m below the surrounding plateaus.

[3] Since 1970, with some interruptions, a cooperative program involving Ethiopia and France has allowed a number of joint studies to be conducted in Afar in various

¹Now at Department of Geology and Geophysics, University of Addis-Ababa, Addis-Ababa, Ethiopia.

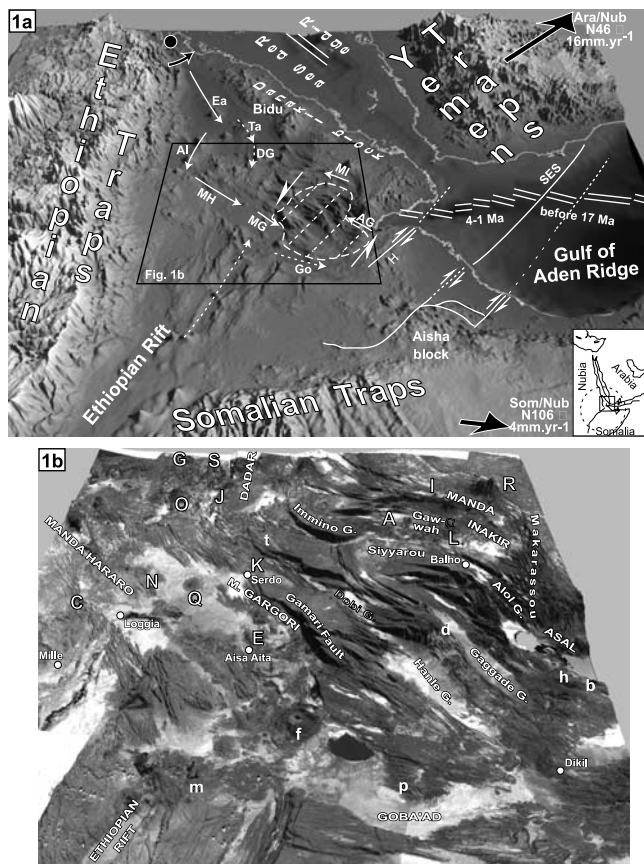


Figure 1. Regional and local Afar morphology. (a) Topographic map of the Afar Depression and major plate boundaries. Double white lines: oceanic ridges. Single white lines: main transform faults from Audin [1999] (H, Holhol; SES, Shukra el Sheik). Black circle and small black arrow: pole and sense of rotation of the Danakil block (from Sichler [1980] and Courtillot et al. [1980]). Large black arrows: relative velocities of the Arabian and Somalian plates (with respect to the Nubian plate [from Jestin and Huchon, 1992]). Full and dashed white arrows: active and incipient propagating rift segments, respectively (AG, Asal-Ghoubbet; Al, Alayta; DG, Dadar Graben; Ea, Erta Ale; Go, Goba'Ad; MG, Manda Gargori; MH, Manda Hararo; MI, Manda Inakir; Ta, Tat'Ali). Half arrow heads and dashed area: overlap zone of Tapponnier et al. [1991, see also Manighetti et al., 1998]. Topography from GTOPO30 database. Lower right inset: position of the Afar triple junction with respect to the main plates (dashed circle: inferred hot-spot boundary). (b) Names of main tectonic and volcanic structures in central Afar. Larger case: main rift segments. Smaller case: main fault systems. Letters: main central volcanoes or centers of silicic activity (all dated in this work, except for small case letters) A, Asa Ale; b, Asa Aleyta; C, Asgura; d, Babba'Olou; E, Borawli; f, Dama Ale; G, Dawa Ale; h, Eger Aleyta; I, Egersuwa; J, Ela; K, Finini; L, Gabalti; m, Gabilema; N, Gablaytu; O, Gad Elu; p, Homor; Q, Kurub Koba; R, Moussa Ali; S, Quarry; t, Undurur. White circle: village or town.

fields of the Earth sciences. Early work in Afar focused on large-scale geologic and structural mapping and, based on conventional K-Ar ages, allowed definition of the main successive volcanic series [Barberi and Varet, 1970, 1977; Barberi et al., 1972, 1975; Gass, 1970; Treuil and Varet, 1973; Varet, 1975; Varet and Gasse, 1978]. These studies provided a first-order picture of the overall evolution of magmatism in the depression, but limited analytical precision of geochronological data prevented more detailed interpretations of Afar rifting. Based on these studies, the geological map of Afar [Varet, 1975] described the spatial distribution of the successive volcanic stages (labeled as "formations"). The so-called Stratoid Series, which is trap-like and mainly basaltic, covers some two thirds of the central AD and yielded ages from ~1 to ~4 Ma [Barberi et al., 1975]. Active rift segments, present within the depression, are now understood in terms of rift propagation [Courtillot et al., 1980] and overlap with both the southern tip of the Red Sea Ridge and western tip of the Gulf of Aden Ridge [Manighetti et al., 1998; Tapponnier et al., 1991]. But understanding the structural significance of the pre-existing Stratoid Series, and the evolution of its potential relationship with the propagators, required additional and more precise age determinations.

[4] Recently, joint studies investigating the structural geology (Audin et al., Paleomagnetic constraints and timing of deformation associated with the onland propagation of the Aden ridge into SE Afar during the last 8 Myr, submitted to *Journal of Geophysical Research*, 2001), paleomagnetism [Kidane, 1999; see also Kidane et al., 2002], and volcanology [Lahitte, 2000] of Afar have provided a significant number of new K-Ar age determinations. All were performed at the Orsay UPS-IPGP laboratory using the Cassinogil-Gillot technique [Gillot and Cornette, 1986]. This paper presents 60 new geochronological measurements [Lahitte, 2000] and proposes a magmatic history of the Central Afar Depression (CAD) over the last 4 Myr. In addition, we have compiled a database including the 250 K-Ar ages available in central Afar in order to investigate the complex relationships of volcanism in the CAD zone. We first describe the space and time distribution of volcanism since 4 Ma at the regional scale. We show that emplacement of the Stratoid Series varied in time and propagated, and describe its transition to the presently active rift segments. Then, we highlight the systematic relation of silicic central volcanoes to rift segment emplacement. This leads us to propose a model of continental rift zone propagation which takes into account these silicic volcanoes and allows us to propose the possible future location of the Aden ridge propagator.

2. Geological Setting

[5] Our study area is located between 10° and 13°N and 40° and 43°E (Figures 1a and 1b), encompassing the CAD and the northernmost extension of the main Ethiopian rift. Volcanic activity in Afar began shortly after eruption of the Ethiopian Traps but apparently was not continuous: the oldest volcanic formation, the Adolei basalts, erupted from 27 to 19 Ma [Barberi et al., 1975; Black et al., 1975; Deniel et al., 1994] and outcrops south of the Ali Sabieh block. The Mabla rhyolites, which now outcrop only on the edges of

the Danakil and Ali Sabieh microblocks (Figure 1b) erupted next, between 16 and 9 Ma [Chessex *et al.*, 1975; Varet, 1975]. This was followed by emplacement of the Dahla basaltic unit from ~8 to ~6 Ma. All the above units outcrop only in a limited area on the southwestern and southeastern margins of the AD. They must originally have occupied a larger area but were since covered by the most important volcanic sequence present in Afar, the Stratoid Series, which outcrops between 40°30' and 42°45'E and 10°30' and 13°N (Figure 2).

[6] The Stratoid Series consists of a pile of meter-decimeter-thick lava flows which covers an area of about 55,000 km² [Varet and Gasse, 1978]. Its total thickness varies spatially and cannot be accurately determined because the base of the sequence is not observed. The largest fault scarps (such as the Gamarri or Hanle faults, Figure 1b) indicate a thickness of at least 1500 m. These lavas, derived from trap-like volcanism, mainly consist of a series of fissural basaltic flows but are underlain by large amounts of silicic lava; several large central volcanoes are also associated with the uppermost part of the lava sequence. The first investigations [Barberi *et al.*, 1975] dated the Stratoid Series ages between 4.4 and 0.4 Ma (based on 37 K-Ar ages). The authors of the geological map [Varet, 1975; Varet and Gasse, 1978] identified a "late Stratoid Series" using intermediate erosional surfaces but recognized the arbitrary nature of this distinction. Courtillot *et al.* [1984] suggested a shorter range, 2.25–1.35 Ma, for the major phase of volcanism (18 K-Ar ages), whereas according to Choukroune *et al.* [1986, 1988] these lavas erupted between 3.5 and 1.25 Ma. The Stratoid Series is contemporaneous with the so-called Tadjoura Series [3.4–1 Ma; Richard, 1979], which outcrops on both sides of the Gulf of Tadjoura and corresponds to the first eruptions from the westward propagation of the Aden Ridge [e.g. Arthaud *et al.*, 1980; Courtillot *et al.*, 1980]. More recently, Zumbo *et al.* [1995] reported ⁴⁰Ar/³⁹Ar age determinations in the Republic of Djibouti ranging between 2.3 and 1 Ma (12 analyses). However, because these studies have different sampling areas, their time ranges cannot be usefully compared. Since 1980, surveying for the 1/100000 scale geological map of the Republic of Djibouti further increased the geochronological database [Dagain *et al.*, 1985; Fournier *et al.*, 1983; Fournier *et al.*, 1984; Fournier and Richard, 1984; Mazet and Recroix, 1986; Richard *et al.*, 1985]. Almost 350 ages are presently available for Afar lavas; more than 250 are from the syn-Stratoid and post-Stratoid volcanism. Sixty of these are new results which we describe in more detail below. Under the classification system of Cox *et al.* [1979], the entire sample suite ranges from basaltic to rhyolitic plotting, on both sides of the tholeiitic-alkaline line [Irvine and Baragar, 1971], forming a transitional suite. This suite as a whole is dominated by basic and acid end-members, with smaller volumes of intermediate compositions (52–63 wt.% of SiO₂) occurring mainly as products of central volcanoes.

3. Geochronology

[7] Samples were selected in order to cover as much as possible the compositional diversity of the CAD. Locations of all new samples are given in Figure 2 and Table 1.

Particular emphasis was placed on previously poorly documented evolved eruptive centers, eight of them being dated here for the first time: they are, from north to south, Dawa Ale, Ela, Egersuwa, Asa Ale, Data Gabalti, Finini, Gablaytu, and Borawli, plus the basaltic volcano of Kurub Koba (Figure 1b). The Ethiopian part of the Manda Inakir rift segment and the Moussa Ali volcano, two key features of the Aden ridge propagator, have been resampled in order to better constrain their volcanic history and local tectonic evolution. Sampling was also focused on some major extensional structures almost devoid of geochronological data: the two southernmost terminations of the Red Sea Ridge system (Manda Hararo and Manda Gargori rift segments), the northwesternmost part of the Stratoid Series and the Gad'Elu volcano, and several zones of transition between the Stratoid Series and active rift segments (Figure 1b). Our sampling, together with complementary sampling by Kidane *et al.* [2002], allows a better coverage of the Ethiopian Stratoid Series within the area corresponding to the geological map of central Afar [Varet and Gasse, 1978]. The proportion of data from the northwestern part of the map has increased from 16% of the total to more than 40%. Nevertheless, some places still suffer from a lack of well-constrained dating, especially north of Immino Graben, south of Goba'ad, and northwest of Asal Lake. Major and trace element geochemical analyses have been performed on the samples dated in this study in Kidane *et al.* [2002] and for the Manda Inakir rift segment in Manighetti *et al.* [1998]. These 105 age and geochemistry coupled analyses are used below to distinguish the age relations of compositionally distinct units. Details of this database can be found in Lahitte [2000].

[8] Volcanic samples were carefully selected in the field to avoid obvious alteration (calcite, zeolite, or any secondary minerals); slightly weathered or vesicular rocks were not collected. Samples suitable for dating were selected following thin-section examinations from a suite of nearly 200 sampled lavas. Due to the (mainly) basaltic nature of Afar lavas, samples often have low potassium concentrations (<1 K%) and display high amounts of atmospheric argon contamination. Most of these are basalts rich in plagioclase phenocrysts within a glassy matrix.

[9] After crushing to obtain the 125–250 micrometer fraction, the selected phase (groundmass or feldspar) was separated using heavy liquids and a magnetic separator. In order to obtain high radiogenic argon contents, measurements are systematically performed on fresh groundmass or K-feldspar rather than on whole rocks. This allows (1) reduction of atmospheric argon contamination; (2) selection of the K-rich groundmasses or minerals; and (3) reduction of the effects of possible extraneous inherited radiogenic argon. Argon isotopic analyses were performed at the UPS-IPGP Geochronology Laboratory at Université Paris Sud, Orsay, using a 180°-sector mass spectrometer [Cassignol and Gillot, 1982]. This equipment is well suited for dating material with minute amounts of radiogenic argon, such as encountered in this study. This technique allows determination of the concentrations of the radiogenic argon down to 0.15% of the total argon extracted [Gillot and Cornette, 1986]. The concentrations of K (determined by atomic absorption) and of Ar are systematically measured at least twice on separate aliquots. The average uncertainty on the K

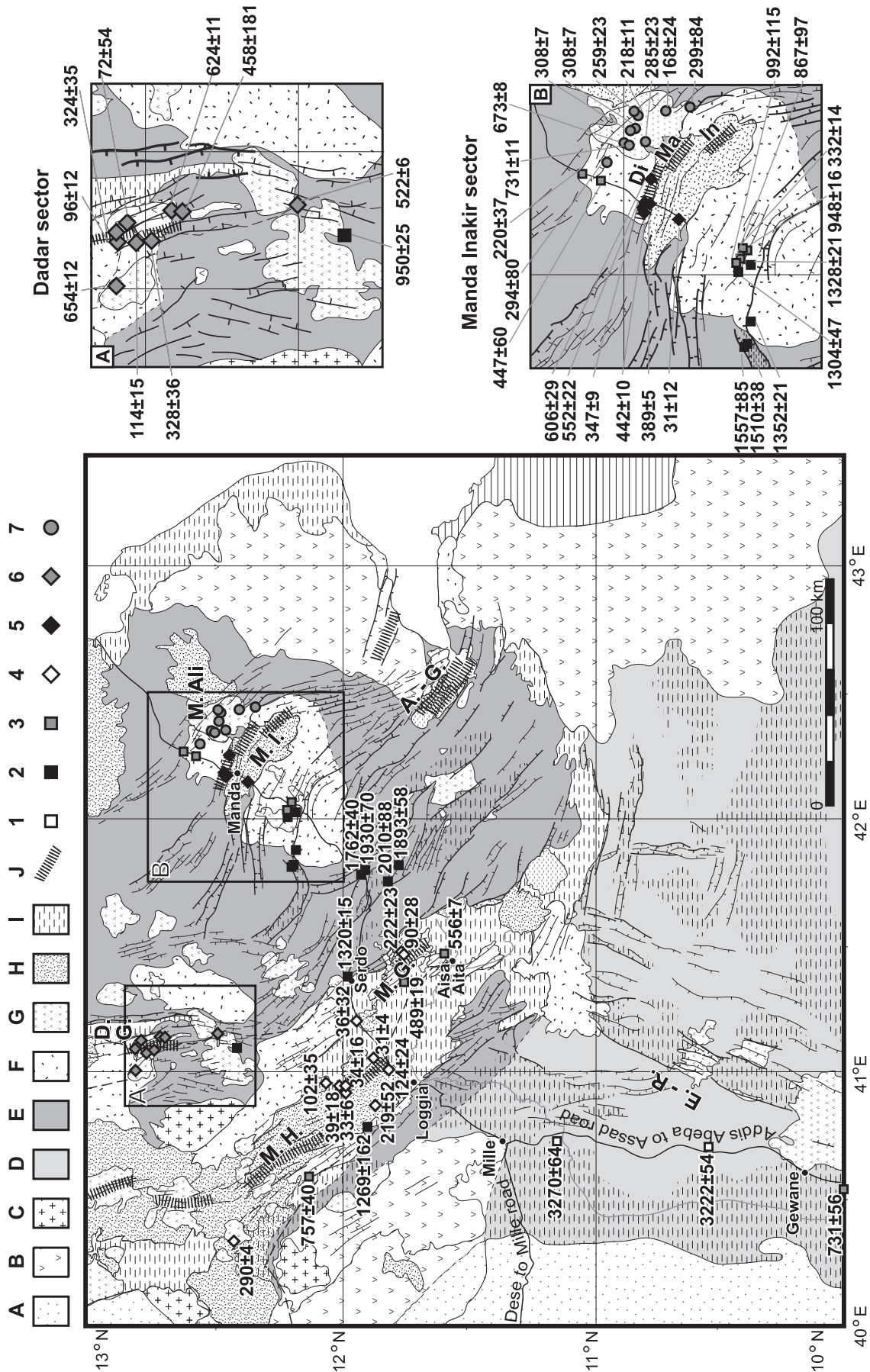


Figure 2. Geological map (modified from *Varret* [1975] and *Kidane et al.* [2002]) and location of the K/Ar ages obtained in this paper (in ka). Main units: (a) pre-Miocene traps and sediments, (b) ante-stratoid volcanism, (c) old granites and associated rhyolites (25 Ma), (d) lower Stratoid Series, (e) upper Stratoid Series, (f) late stratoid volcanism (“Gulf Basalts”), (g) syn-Stratoid and post-Stratoid silicic volcanism, (h) basaltic volcanism of the rift segments, (i) Quaternary sediments, (j) Recent volcano-tectonic axes. Assignment of samples: (1) lower Stratoid Series, (2) upper Stratoid Series, (3) late stratoid volcanism (“Gulf Basalts”), (4) Manda Hararo rift segment, (5) Manda Inakir rift segment, (6) Dadar Graben, (7) Moussa Ali volcano. In, Inakir rift segment; Ma, Manda rift segment; Di, Dirko Koma rift segment.

Table 1. New K-Ar Results^a

Sample and Rock Type ^b	Longitude and Latitude	K, ^c %	Sample Mass, g	⁴⁰ Ar*, ^d %	⁴⁰ Ar*, ^c 10 ¹² atoms/g	Age, ^{f,g} Ma	1σ, ^{g,h} Ma
<i>Lower Stratoid Series Unit</i>							
75CB1	40.713	0.731	1.02	8.18	2.52	3.308	0.071
B	11.129		0.58	10.63	2.47	3.241	0.058
Upper flow of the lower Stratoid Series along the Awash river						3.270	0.064
75CC	40.709	0.730	0.51	11.26	2.35	3.082	0.054
B	10.535		0.75	12.58	2.55	3.346	0.055
Flat top of the southwestern Stratoid Series (50 km north of Gewene)						3.222	0.054
<i>Upper Stratoid Series Unit</i>							
75B1	41.759	1.123	1.03	3.33	2.43	2.072	0.096
B	11.803		0.32	3.74	2.29	1.954	0.081
Basal flow of the southeastern fault scarp of Dobi Graben						2.010	0.088
75AJ2	41.784	0.561	0.96	4.40	1.11	1.902	0.068
B	11.908		0.80	4.24	1.14	1.959	0.073
Intermediate flow of the northern scarp of Dobi Graben						1.930	0.070
75D	41.823	0.668	1.02	5.00	1.27	1.830	0.059
B	11.760		0.64	5.58	1.36	1.950	0.057
Basal flow of the southeastern fault scarp of Dobi Graben						1.893	0.058
75AJ1	41.785	1.007	1.00	7.85	1.90	1.809	0.040
B	11.909		0.86	7.28	1.80	1.711	0.040
Upper flow of the northern scarp of Dobi Graben						1.762	0.040
75AE2	41.816	0.687	0.98	2.67	1.09	1.532	0.094
B	12.184		0.49	3.57	1.13	1.575	0.077
Lower flow on the northeastern fault of Immino Graben						1.557	0.085
75AE1	41.816	0.774	0.52	5.74	1.22	1.518	0.043
B	12.184		0.53	7.76	1.21	1.505	0.034
Lower flow on the northeastern fault of Immino Graben						1.510	0.038
75AF	41.883	2.612	0.50	15.04	3.70	1.357	0.020
R	12.167		0.51	14.15	3.67	1.347	0.021
Lower flow on the southeastern fault of Immino Graben						1.352	0.021
75BK	42.032	1.625	0.62	14.01	2.27	1.338	0.021
T	12.167		1.00	13.66	2.23	1.319	0.021
SE pyroclastic flow of the Asa Ale volcano on Gawwah plateau						1.328	0.021
75BP	42.023	2.030	0.90	4.75	2.80	1.322	0.044
T	12.200		0.48	5.34	2.85	1.346	0.041
			0.53	5.43	2.77	1.308	0.039
Lava flow inside the caldera of Asa Ale volcano on Gawwah plateau						1.325	0.041
75BY1	41.382	3.593	1.17	54.71	4.94	1.318	0.015
O	11.962		1.38	60.48	4.95	1.321	0.015
Internal dome of the Sardo unit						1.320	0.015
75AL	40.788	0.418	1.07	1.17	0.52	1.194	0.158
B	11.884		0.72	1.26	0.58	1.339	0.165
Flow recovering the silicic dome of Loggia unit						1.269	0.162
<i>Gulf Basalts</i>							
75BN	42.024	0.688	0.99	1.04	0.71	0.992	0.143
B	12.200		0.47	1.55	0.71	0.992	0.096
Inside the Asa Ale caldera, upper flow on the easternmost fault scarp of the Immino Graben						0.992	0.115
72S	41.100	4.093	1.00	6.17	4.02	0.940	0.026
R	12.400		0.99	7.36	4.09	0.957	0.024
Flow interstratified in the upper part of the Stratoid Series						0.950	0.025
75AD2	42.072	3.115	0.84	10.52	3.11	0.958	0.017
T	12.184		0.82	13.06	3.06	0.941	0.015
Small Dome on the Gawwah plateau						0.948	0.016
75BM	42.026	0.769	1.02	1.70	0.65	0.817	0.073
B	12.197		0.50	1.05	0.76	0.947	0.135
Inside the Asa Ale caldera, intermediate flows on the easternmost fault scarp of the Immino Graben						0.867	0.097
75AO	40.591	0.449	1.00	3.19	0.36	0.781	0.038
B	12.115		1.28	2.65	0.34	0.728	0.042
Flow on the SE margin of the CMH sensu stricto rift segment						0.757	0.040
75A	41.473	3.198	0.75	23.88	1.85	0.555	0.007
O	11.580		1.44	31.26	1.86	0.557	0.007
Southernmost flow of Borawli volcano						0.556	0.007
72A	41.430	1.078	1.00	3.20	0.55	0.489	0.024
B	11.620		1.00	3.73	0.54	0.488	0.021
			1.50	5.16	0.55	0.490	0.015
Flow at north of Aisa Ayta (SE of Borawli volcano)						0.489	0.019

Table 1. (continued)

Sample and Rock Type ^b	Longitude and Latitude	K, ^c %	Sample Mass, g	⁴⁰ Ar*, ^d %	⁴⁰ Ar*, ^e 10 ¹² atoms/g	Age, ^{f,g} Ma	1 σ , ^{g,h} Ma
75AC	42.072	0.557	1.02	3.12	0.18	0.310	0.015
B	12.184		1.94	4.31	0.20	0.349	0.013
Upper flow of the Gawwah plateau						0.332	0.014
<i>Manda Hararo Rift Segment</i>							
80AE3	40.329	3.591	1.10	23.10	1.11	0.290	0.004
O	12.389		1.43	34.07	1.10	0.289	0.003
Flow from flank of Badi volcano						0.290	0.004
75AK	40.873	0.095	0.83	0.15	0.00	0.093	0.090
B	11.853		2.10	0.81	0.02	0.243	0.045
Flow on the SE flank of the CMH sensu stricto rift segment						0.219	0.052
72G1	41.014	0.762	1.01	0.75	0.09	0.115	0.023
B	11.800		1.13	0.80	0.10	0.133	0.025
Flow on the SE flank of the CMH sensu stricto rift segment						0.124	0.024
70R	40.946	0.858	1.08	0.47	0.11	0.125	0.040
B	12.045		0.96	0.37	0.06	0.073	0.029
Flow of the Unda Hararo volcano faulted by Manda Hararo NE faults						0.102	0.035
70O	40.950	0.592	0.50	0.10	0.036	0.059	0.087
B	11.995		0.99	0.03	0.011	0.017	0.091
TL age ⁱ		48 ± 22		816 ± 72		0.039	0.019
Upper flows of the Dora volcano, affected by the northeastern recent fault of the axial Manda Hararo sensu stricto rift segment						0.039	0.018
72F	41.207	0.510	1.47	0.20	0.02	0.040	0.030
B	11.927		1.02	0.03	0.00	0.010	0.044
Easternmost flow of the Kurub Koba volcano						0.036	0.032
70P	40.945	0.608	1.07	0.25	0.19	0.301	0.183
B	11.990		1.00	0.29	0.20	0.309	0.158
TL age ⁱ		40 ± 20		801 ± 70		0.032	0.016
Upper flows of the Dora volcano, affected by an axial recent fault of the Manda Hararo sensu stricto rift segment						0.034	0.016
70Q	40.940	0.520	1.00	0.26	0.09	0.171	0.099
B	11.985		1.01	0.10	0.03	0.059	0.093
TL age ⁱ		24 ± 4		733 ± 58		0.033	0.006
Upper flows of the Dora volcano, affected by the southwestern recent fault of the axial Manda Hararo sensu stricto rift segment						0.033	0.006
70V	41.060	2.496	1.00	1.01	0.08	0.031	0.005
O	11.860		1.00	1.16	0.08	0.031	0.004
Flow from a fault scarp inside Gablaytu volcano						0.031	0.004
<i>Manda Gargori Rift Segment</i>							
70D	41.480	0.845	1.01	1.62	0.20	0.229	0.021
B	11.750		1.12	1.27	0.18	0.213	0.025
Upper flow on internal fault scarp of the Manda Gargori rift segment						0.222	0.023
70A	41.470	0.524	2.00	0.17	0.02	0.041	0.036
B	11.740		2.00	0.60	0.05	0.104	0.026
Upper flow on southeastern external fault scarp of the Manda Gargori rift segment						0.090	0.028
<i>MI Rift Segment</i>							
75AB	42.258	0.625	1.13	3.49	0.38	0.586	0.026
B	12.430		1.26	3.05	0.41	0.630	0.032
Upper flow of the northern fault of the Dirko Koma rift segment						0.606	0.029
75G	42.189	0.849	1.04	3.58	0.49	0.561	0.024
B	12.451		1.00	4.32	0.48	0.544	0.020
Basis of the northeastern fault scarp of Dirko Koma rift segment						0.552	0.022
75BW	42.254	0.883	1.02	1.22	0.44	0.487	0.060
B	12.562		0.97	1.00	0.36	0.398	0.059
Spatter cone on the Manda range, north to Dirko Koma rift segment						0.447	0.060
75I1	42.176	3.987	0.95	8.68	1.83	0.440	0.009
R	12.445		0.49	7.30	1.84	0.444	0.010
Internal dome of Egersuwa volcano						0.442	0.010
75J2	42.178	3.564	0.99	26.11	1.45	0.391	0.005
O	12.440		0.99	27.54	1.44	0.388	0.005
External SE flow of Egersuwa volcano						0.389	0.005
75H	42.174	1.250	0.99	5.56	0.46	0.355	0.010
B	12.444		1.53	6.79	0.44	0.341	0.008
Terminal flow at the summit of Egersuwa						0.347	0.009
75BV	42.272	0.635	1.00	0.88	0.15	0.221	0.038
B	12.611						

Table 1. (continued)

Sample and Rock Type ^b	Longitude and Latitude	K, ^c %	Sample Mass, g	⁴⁰ Ar*, ^d %	⁴⁰ Ar*, ^e 10 ¹² atoms/g	Age, ^{f,g} Ma	1σ, ^{g,h} Ma
External flow on the northern basement of the young Manda range						0.221	0.038
75V	42.152	0.836	1.40	0.22	0.01	0.020	0.014
B	12.357		1.93	0.46	0.03	0.035	0.011
External flow on the southern slope of Manda range						0.031	0.012
<i>Dadar Graben</i>							
75AY	41.011	3.107	0.99	10.26	2.10	0.649	0.012
O	12.801		1.00	10.03	2.13	0.659	0.012
Flow on northern slope of Dawa Ale volcano						0.654	0.012
75AR	41.144	2.773	1.01	10.97	1.80	0.624	0.011
T	12.704		1.03	11.18	1.80	0.624	0.011
Dome in the middle part of the eastern fault scarp of Dadar Graben						0.624	0.011
75BI	41.157	3.909	0.68	29.93	2.11	0.518	0.006
O	12.476		1.10	32.51	2.14	0.525	0.006
External southwestern flow of the many-faulted Ela volcano						0.522	0.006
75AQ	41.145	0.703	1.13	0.40	0.34	0.470	0.175
B	12.698		0.53	0.35	0.32	0.446	0.187
Flow on the upper part of the easternmost Dadar Graben fault						0.458	0.181
75AZ	41.096	0.451	1.54	1.17	0.18	0.376	0.049
B	12.742		1.42	0.97	0.15	0.311	0.048
TL age ⁱ		801±66		245±37		0.306	0.052
Hyaloclastite cone on the western margin of the Dadar Graben						0.328	0.036
75BC	41.112	0.613	1.26	1.34	0.20	0.319	0.036
B	12.786		1.08	1.47	0.21	0.329	0.034
Flow on the northernmost part of the axial eastern Dadar Graben fault						0.324	0.035
75BB	41.106	0.348	0.74	0.19	0.09	0.239	0.184
B	12.756		0.84	0.20	0.09	0.228	0.180
TL age ⁱ		68 ± 6		604 ± 59		0.113	0.015
Upper flow in the central part of the axial western Dadar Graben fault						0.114	0.015
75AS1	41.107	0.370	1.00	0.25	0.04	0.113	0.068
B	12.794		0.99	0.22	0.04	0.104	0.071
TL age ⁱ		86 ± 4		898 ± 101		0.096	0.012
Flow on the northernmost part of the axial western Dadar Graben fault						0.096	0.012
75BE	41.125	0.512	1.18	0.21	0.04	0.077	0.054
B	12.785		1.16	0.18	0.03	0.066	0.053
Flow on the northernmost part of the eastern Dadar Graben fault						0.072	0.054
<i>Moussa Ali Volcano (M. Ali)</i>							
75N	42.357	0.931	1.98	18.59	0.70	0.728	0.010
B	12.482		1.81	14.73	0.71	0.735	0.011
Flat top of the first stage of M. Ali						0.731	0.011
75K	42.348	3.488	1.02	30.78	2.44	0.672	0.008
R	12.488		1.04	22.28	2.45	0.674	0.009
Flow on the eastern flank of the first stage of M. Ali						0.673	0.008
75O	42.391	1.246	1.42	7.81	0.40	0.311	0.007
B	12.472		1.90	7.72	0.39	0.305	0.007
Flow on the summit slope of M. Ali						0.308	0.007
75P1	42.394	2.219	1.01	9.04	0.71	0.307	0.006
TB	12.471		1.00	7.22	0.71	0.309	0.007
Near the summit of M. Ali						0.308	0.007
55AF	42.448	1.242	1.07	0.41	0.30	0.231	0.083
B	12.328		0.52	0.60	0.44	0.345	0.085
Upper flow on the southeastern slope of the third stage of M. Ali						0.299	0.084
75S	42.303	0.609	1.02	0.51	0.13	0.216	0.064
B	12.547		1.00	0.57	0.23	0.362	0.094
Flow on the easternmost slope of the M. Ali						0.294	0.080
75BT	42.358	3.611	0.28	2.27	1.10	0.293	0.020
T	12.444		0.30	1.44	1.02	0.272	0.029
Flow from a dome on southern slope of the second stage of M. Ali						0.285	0.023
55AD	42.426	2.006	1.00	3.77	0.59	0.285	0.012
TB	12.464		1.00	4.41	0.49	0.238	0.009
			0.99	3.51	0.53	0.257	0.012
Upper flow of the eastern slope of the second stage of M. Ali						0.259	0.023
55AC	42.425	1.550	1.00	2.66	0.34	0.214	0.012
B	12.460		1.03	3.42	0.35	0.222	0.010
Lower flow on the eastern slope of the third stage of M. Ali						0.218	0.011
55AB	42.439	0.460	1.61	0.96	0.08	0.176	0.027

Table 1. (continued)

Sample and Rock Type ^b	Longitude and Latitude	K, ^c %	Sample Mass, g	⁴⁰ Ar*, ^d %	⁴⁰ Ar*, ^e 10 ¹² atoms/g	Age, ^{f,g} Ma	1σ, ^{g,h} Ma
TB	12.402		1.51	1.11	0.07	0.161	0.020
Upper flow on the southeastern slope of the third stage of M. Ali							
<i>Abida Central Volcano</i>							
75CF	40.541	0.524	0.63	2.20	0.41	0.761	0.052
B	9.978		1.11	1.76	0.37	0.692	0.059
Flow on the southeastern slope of Abida volcano (Ethiopian rift)							
						0.731	0.056

^aResults of K-Ar dating of 60 lava flows from the AD.

^bB, basalt; TB, trachy-basalt; T, trachyte; R, rhyolite; O, obsidian.

^cWeight percentage of potassium in sample.

^dPercentage of radiogenic argon 40 in sample.

^eNumber of atoms of radiogenic argon 40 per gram of sample.

^fAges determined from at least two replicate argon measurements for each sample.

^gThe means of replicate determinations are given in bold.

^hUncertainties.

ⁱThermoluminescence determination, paleodose (in Gy) and annual dose rate (in μGy/a) are given (see *Lahitte et al.* [2001] for details).

and Ar concentrations is about 1% [*Gillot and Cornette*, 1986]. The interlaboratory standards MDO-G, ISH-G, and GL-O, as well as atmospheric Ar, were used to calibrate the analyses [*Gillot et al.*, 1992; *Odin*, 1982]. Details of the analytical methods are described elsewhere [*Gillot and Cornette*, 1986]. Age calculations are based on ⁴⁰K abundance and decay constants recommended by *Steiger and Jager* [1977].

[10] Six samples, suffering from insufficiently precise K-Ar ages (Table 1 and *Lahitte et al.* [2001]), were also analyzed using the thermoluminescence technique proposed by *Valladas et al.* [1978, see also *Guerin and Valladas*, 1980]. This technique had been shown to be suitable for dating basaltic rocks up to 0.5 Ma [*Gillot and Cornette*, 1986]. The age corresponds to the ratio between the sample paleodose (total natural radiation dose, which the lava received since cooling, proportional to the light emitted by laboratory heating) and its annual dose rate (depending on the α, β, and γ emissions calculated from U, Th, and K concentrations [*Lahitte et al.*, 2001]). The thermoluminescence (TL) glow is measured at high temperature (from 500°C and up to 700°C) on minerals which have part of their spectral emission in the ultraviolet region. This allows minimizing anomalous lower temperature fading [*Wintle*, 1973] and the red light perturbation of the heating plate. We used plagioclase microliths extracted from samples by the usual crushing, sieving, and heavy-liquid separation, as suggested by *Guerin and Valladas* [1980].

4. Results

[11] K-Ar ages are presented in Table 1 and grouped according to the main features of the CAD: lower and upper stratoid formations [as defined by *Kidane et al.*, 2002], Gulf Basalts, Manda Hararo-Manda Gargori, Manda Inakir, and Dadar Graben rift segments, and Moussa Ali volcano (see Figures 1b and 2, and also Table 1 for a description of the sampling context).

[12] The lower stratoid formation outcrops between the villages of Mile and Gewane and ranges in age from 3.3 to 2.6 Ma [see also *Kidane et al.*, 2002]. Only three dated samples (all in the basic field), are available for this unit, two from the present study (75CB1 and 75CC, Table 1). All

other samples from this study are located north of Mile (Figure 2) and are younger than 2.0 ± 0.1 Ma.

[13] The upper stratoid formation covers a wide part of the CAD, mainly to the north and east of the Manda Hararo-Goba'ad rift zone but also in a narrow band along the southwestern border of this rift zone. The 11 sampled flows occur in 4 main clusters: 2 on both the SW and NE borders of the Manda Hararo rift zone (75AL, 75BY1 respectively), 4 inside (75B1, 75D) and to the north (75AJ1, 75AJ2) of the Dobi Graben, 3 at the base of Immino Graben faults (75AE1, 75AE2, 75AF), and 2 near the top (75BK, 75BP). They all yield ages in agreement with the interval obtained by *Kidane et al.* [2002] for this unit (i.e., 1.36 ± 0.11 to 2.08 ± 0.08 Ma). The 36 dated flows are categorized as follows: 86% are basic, 3% are intermediate, and 11% are acidic.

[14] The Gulf Basalts volcanic unit (also called Recent Basalts) is poorly defined. It corresponds to the uppermost part of the trap-like formation which mainly outcrops on the margins of the presently active rift segments. We obtained six ages from this volcanic unit in three distinct areas:

- The first area represents the margin of Manda Hararo rift segment. Considering ages ranging between 0.59 ± 0.16 and 1.11 ± 0.09 Ma, *Kidane et al.* [2002] suggested that these lava flows located along the northeastern margin of the Manda Hararo rift segment (Serdo-Semera block) could be identified as Gulf Basalts, whereas they were previously associated with the Stratoid Series by *Varet et al.* [1978]. Our new age (72S, 0.95 ± 0.02 Ma) is consistent with this reinterpretation. Furthermore, the same change can be applied along the SW margin of this rift segment. Indeed, 75AO (0.76 ± 0.04 Ma, Table 1) is in agreement with this interpretation. Both the NE and SW margins of the Manda Hararo rift segment present the same aspect with meter-decameter-thick lava flows, presently tilted $10^\circ \pm 5^\circ$ toward N235°W and N55°E, respectively.

- The second area is the western margin of the Manda Gargori rift segment, where basaltic lavas yielded three ages ranging from 0.49 ± 0.02 to 0.65 ± 0.10 Ma (72A and 75A in Table 1 and *Kidane et al.* [2002]).

- The third area, the Gawwah plateau, is located to the north of the Siyyarou plateau, which was defined as a tectonic block by *Kidane et al.* [2002]. The three new ages range from 0.85 ± 0.10 to 1.00 ± 0.10 Ma (75AD2, 75BM,

75BN, Table 1), in agreement with those obtained by these authors on the Siyyarou block (ranging from 0.85 ± 0.02 to 0.94 ± 0.10 Ma) and with the one obtained by *Manighetti et al.* [1998], i.e., 0.89 ± 0.06 Ma, near Balho village on the northeastern scarp of Alol Graben (Figure 1b). Furthermore, according to Spot image analysis and field observations, these lavas display the same morphologic character as the Gulf Basalts in the Siyyarou and Gawwah plateaus. We also interpret these blocks as part of a single one (Siyyarou-Gawwah unit), fractured by faults at a previous stage of propagation of the Aden Ridge. Further, we expand, in this sector, the eastern limit of Gulf Basalts unit to the area, previously associated with the Stratoid Series by *Varet et al.* [1978], located east of the Siyyarou-Gawwah plateau and south of the Inakir range (Figure 2). A late lava flow (75AC), which partially seals fault scarps that separates the Siyyarou and Gawwah plateaus, has been dated at 0.330 ± 0.014 Ma. We therefore constrain the dismantling of the Siyyarou-Gawwah unit and corresponding rift propagation stage around 0.35 to 0.85 Ma.

[15] Whereas the Gulf Basalts unit was the smallest basaltic one in extent on the geological map of *Varet et al.* [1978], our reinterpretations, and those proposed by *Kidane et al.* [2002], widely extend the area covered by this unit to the margins of presently active rift zones. This now defines a transition between the Stratoid Series and the presently active rift segment. The 14 dated flows are categorized as follows: 71% are basic, 7% are intermediate, and 21% are acidic.

[16] Prior to our study, age relations in the Manda Hararo-Goba'ad rift zone were poorly documented. With 10 new ages (Table 1), this structure can now be better described. All but one age (70V, acid lava) come from basaltic lavas. Seven of them [*Lahitte et al.*, 2001] come from the Manda Hararo rift segment *sensu stricto* and range from 0.031 ± 0.004 to 0.22 ± 0.05 Ma (70V, 70Q, 70P, 70O, 70R, 72G1, 72AK, Table 1). The age, location, and basaltic nature of the small Kurub Koba central volcano link it to this unit (0.036 ± 0.032 Ma, 72F, Table 1).

[17] Manda Gargori, the youngest propagator that can be linked to the Red Sea Ridge, is constrained by only two ages at 0.09 ± 0.03 and 0.22 ± 0.02 Ma (70A, 70D, Table 1), from tholeiitic basalts. Although no historical activity has been reported, there is evidence (such as footprints in a fresh ash fall deposit, observed by one of us, PYG) that its last activity is recent. Considering ages available for the Gulf Basalts, located at the margins of the Manda Hararo rift segment, continuity of volcanism since 1 Ma can be inferred in this area. Furthermore, volcanic activity on both the Manda Hararo and Manda Gargori rift segments is very young and located near the presently most active rift zone.

[18] Based on data collected in the Republic of Djibouti, the Manda Inakir has been suggested to be the most recent rift segment that can be associated with Aden Ridge propagation [*Manighetti et al.*, 1998]. In order to complete the study of this rift, we have analyzed eight samples collected on the Ethiopian side. Seven of them, which come from the margin of the presently active rift segment, produced ages ranging from 0.22 ± 0.04 to 0.61 ± 0.03 Ma (75BV, 75G, 75H, 75I1, 75J2, 75BW, 75AB, Table 1). Sample 75V comes from the Manda shield volcanic struc-

ture and provides an age of 0.031 ± 0.012 Ma. The 19 dated flows are categorized as follows: 79% are basic (mostly alkaline), 11% are intermediate, and 11% are acidic.

[19] The Dadar Graben is the southernmost tectonic feature of the Erta Ale-Tat'Ali eastern propagation path of the Red Sea Ridge (Figure 1a). The central floor, affected by a system of normal faults striking approximately 150° , yields five ages ranging from 0.07 ± 0.05 to 0.33 ± 0.04 Ma (75AS1, 75AZ, 75BB, 75BC, 75BE, Table 1), whereas its lateral margins, 150 m above the central floor, yield four ages from 0.46 ± 0.18 to 0.65 ± 0.01 Ma (75AR, 75AQ, 75AY, 75BI, Table 1). Three dated samples are rhyolitic lavas (75AY, 75BI, 75AR); others are tholeiitic basalts.

[20] Ten samples from the Moussa Ali volcano provide ages from 0.17 ± 0.02 to 0.73 ± 0.01 Ma (55AB, 55AC, 55AD, 75BT, 75S, 55AF, 75P1, 785O, 75K, 75N, Table 1), in agreement with previous studies [*Civetta et al.*, 1974; *De Fino et al.*, 1973; *Zumbo et al.*, 1995]. Within this interval, two periods of volcanism can be identified; one before 0.6 Ma and another after 0.35 Ma. Furthermore, field investigations suggest that the base could even be a few hundred thousand years older. The dated flows are slightly alkaline and categorized as follows: 45% are basic, 36% are intermediate, and 18% are acidic.

[21] Finally, basaltic sample 75CF (Figure 2), taken on an external lava flow of the polyphase Abida central volcano near Gewane village, has been dated at 0.73 ± 0.06 Ma (Table 1). This is our southernmost sample, close to the western margin of the EAR.

[22] Four of the six results obtained from TL measurements are compatible with K-Ar ones (70O, 75AS1, 75AZ, 75BB, Table 1), with better precision ($\pm 20\%$). Two samples (70P and 70Q) have incompatible K-Ar and TL ages (Table 1). Nevertheless, their more precise TL ages are consistent with results obtained on other neighboring samples (see for instance the well-constrained K-Ar age of sample 70V and the TL and K-Ar ages of sample 70O, which correspond to the same volcanic activity [*Lahitte et al.*, 2001]). We conclude that these TL ages are reliable.

5. Space-Time Distribution of Plio-Quaternary Volcanism

5.1. Available Geochronological Data

[23] In addition to the results described above and in Table 1, a large number of ages obtained with the K-Ar method are now available for the CAD. Most have been obtained by the K-Ar technique; only a few were obtained using ^{40}Ar - ^{39}Ar . In order to take into account only the best-constrained data, we decided to base our selection on reported uncertainties. Because conventional K-Ar analyses typically display large uncertainties, we decided to exclude the 16 ones which have both an uncertainty larger than 200 ka and a relative uncertainty worse than 35%; the resulting filtered data display an average precision of 200 ka. We have considered all ages for the Stratoid Series (130 data), excluding those which presented an obvious incompatibility with better-constrained results. In order to describe in detail which rift segments were active during the last 1 Myr, only Cassinot-Gillot technique ages and the few $^{40}\text{Ar}/^{39}\text{Ar}$ ages reported by *Zumbo et al.* [1995] have been considered. With

this selection, about 230 ages can be used to reconstruct the volcanic evolution of the CAD in the last 4 Myr:

- Sixty new results (this work, Table 1) obtained using the Cassagnol-Gillot technique have an average uncertainty of 37 ka.
- Eighty-one previous ages obtained using the Cassagnol-Gillot technique have an average uncertainty of 64 ka. They come from *Manighetti et al.* [1998] (24 ages), *Kidane et al.* [2002] (30 ages), and *Audin* [1999] (2 ages); one of us (PYG) performed 25 unpublished age determinations for the Abhe Bad, Ali Sabieh, Dikil, Djibouti, Loyada, and Tadjoura sheets of the 1:100,000 geological map of Djibouti [*Dagain et al.*, 1985; *Fournier et al.*, 1983; *Fournier et al.*, 1984; *Fournier and Richard*, 1984; *Mazet and Recroix*, 1986; *Richard et al.*, 1985].
- Seventy-three ages obtained with conventional K-Ar techniques have an average accuracy of 256 ka: *Barberi et al.* [1972] (6 ages), [1974] (23 ages); *Civetta et al.* [1974] (9 ages); *Richard* [1979] (13 ages); *Gasse et al.* [1980] (2 ages); *Courtillet et al.* [1984] (15 ages); and B.R.G.M. K-Ar laboratory in Orléans (5 unpublished ages on the Loyada sheet). Ages obtained before the definition of the currently used ^{40}K abundance and decay constants have been recalculated using them.
- Twelve ages have been performed using the ^{40}Ar - ^{39}Ar incremental heating technique by *Zumbo et al.* [1995]. Their average precision is 95 ka.

5.2. Volcanic Activity Through Time

[24] All new K-Ar ages obtained here (Table 1) range from 3.5 Ma to the present. Because we did not sample the base of the lower Stratoid Series (especially the south of Goba'ad Graben), our time interval is shorter than the one previously proposed by *Barberi et al.* [1972]. All ages critically assessed and compiled in the previous section have been plotted as a function of time in Figure 3a and then in Figure 4 in order to outline any geographical concentration in the distribution. To first order, the distribution appears to follow two linear segments (Figure 3a), implying a succession of two periods with uniform distribution, with a change in characteristics at about 2.3 Ma. Prior to this date, the mean delay between two consecutive data is 43 ± 18 kyr, whereas it becomes three to four times less, i.e., 13 ± 5 kyr, after it. Each datum has been modeled as a unit surface normal (Gaussian distribution) with standard deviation equal to the analytical uncertainty. The resulting integrated curve is shown in gray at the bottom of Figure 3b. Although it indeed approximates a step function, with the step near 2.3 Ma, second-order variations are seen, with high-amplitude high-frequency variations at the younger end and a secondary maximum at about 2 Ma.

[25] The older part of the distribution, prior to 2.3 Ma, indicates either lesser volcanic activity or under-sampling of the older formations. It is clear that the older formations (e.g., the lower stratoid and the Dahla formations) continue underneath the widespread coverage by the upper Stratoid Series, which has flooded most of the AD. No dated drill-core material is available in central Afar. It is therefore difficult to establish an unquestionable relationship between total volume erupted and time, particularly for the lower Stratoid Series. However, surface outcrops, fault exposures, and morphological observations all emphasize the very

large volume of the Upper Stratoid Series and its trap-like appearance. The Gamarii fault, with more than 1000 m of lava erupted between 2.3 and 1.6 Ma, illustrates well this increase in the volume of discharge [*Kidane et al.*, 2002]. It is therefore likely that the break in slope in Figure 3a does reflect a genuine change in volcanic productivity.

[26] *Courtillet et al.* [1984], followed by *Manighetti et al.* [1998] and to a lesser extent by *Kidane et al.* [2002], had suggested (based on a far more limited database) that a pulse of magmatism occurred around 2 Ma and a minor one about 1 Ma and that volcanism in general had been episodic, alternating with periods dominated by tectonic activity. Figure 3 does not confirm this scenario to first order but rather emphasizes a remarkable continuity of volcanic activity all the way to the present. Peaks in the distribution may be related to oversampling of formations; such could be the case for the most recent products linked to the active rift segments. Indeed, volcanism in Afar seems to have evolved from a diffuse, widespread style, generating a trap-like series, to more concentrated activity on propagating rift segments localized toward the margins of the depression.

[27] Because the distribution in Figure 3a makes no reference to the actual volumes represented by our samples and in order to minimize the potential effects of under-sampling of the older flows, we have attempted to correct this bias in the following way. We define "elementary boxes" corresponding to square surfaces $12'$ of arc on the side and having time periods of 0.2 Myr. Time, latitude, and longitude limits are 4 to 0 Ma, 10° – 13°N , and 40° – 43°E , respectively. We consider only those boxes which contain one or more datum. For each period of time, we assume that the importance of volcanic activity is related to the size of the area covered, i.e., to the number of elementary boxes recording activity. The resulting distribution is shown as a black dotted curve at the bottom of Figure 3b. It is reasonably similar to the uncorrected, raw distribution, but some finer features emerge. Independent from the possible under-estimation of volcanic activity before 2.3 Ma, the peak in the distribution at ~ 2 Ma is enhanced and becomes the most prominent feature of the last 3 Ma, on top of the step-like distribution. A secondary peak is found at ~ 1.3 Ma, with secondary minima at 1.7 and 0.9 Ma. There is no confirmation of unusually intense increase in activity in the last 0.5 Myr. The bias-corrected maxima correspond to the events outlined by *Courtillet et al.* [1984], who indeed sampled more lava flows in these age ranges. But these maxima in volcanic activity have an amplitude of no more than 2 with respect to minima and hence do not correspond to exceptional pulses. Our analyses, based on 10 times more data and much wider coverage underline continued activity in Afar since 3.5 Ma (at least with the Dahla and Mabla formations emplaced prior to that) and a significant phase of increased volcanic activity at ~ 2.3 Ma and continuing since, with 100% modulations and maximum flux at ~ 2 Ma.

5.3. Emplacement of Stratoid Series in Space and Time

[28] The previous analysis assumes that time is the only relevant free parameter, without taking into account the possible lack of spatial homogeneity of the data. Indeed, we are aware of the lateral rift propagation which occurs in the studied area. Lack of proper exposure of the Stratoid Series,

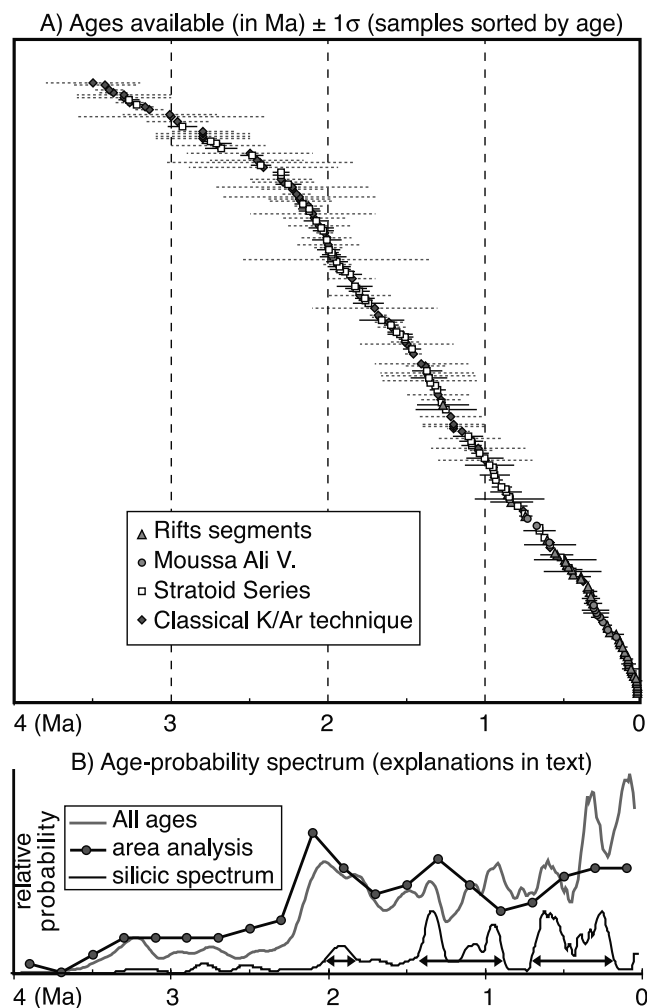


Figure 3. Compilation of all available ages in central Afar. (a) Ages sorted from oldest to youngest with their 1σ uncertainty. Triangles, circles, squares with solid lines: rift segments, Moussa Ali volcano, and Stratoid Series ages, dated by Cassagnol-Gillot technique. Diamonds with dashed line: Stratoid Series dated by other techniques. (b) Age-probability spectra. gray curve, all dated rocks; thin black curve, silicic volcanism only; thick black curve, distribution weighted by area (see text).

particularly in vertical section, despite numerous fresh fault scarps, prevents us from constraining precisely the onset and, to a certain degree, the extent of the formation.

[29] Examination of the entire age database shows that the barycenter of our 19 lower Stratoid Series samples, 65 upper Stratoid Series, and 54 Gulf Basalt samples appears to roughly migrate northward [Lahitte, 2000]. However, several samples in our compilation have ages with poor precision or are not compatible with well-constrained, newer age determinations: for instance, *Barberi et al.* [1975] dated the base and the top (1000 m higher) of the Gamarii fault scarp at 3.9 ± 0.3 and 3.3 ± 0.1 Ma, respectively. *Kidane et al.* [2002] obtained five K-Ar ages at the bottom of this section, all ranging between 2.0 and 2.3 Ma, with an accuracy better than 0.1 Myr. North of the Asal lake, *Barberi et al.* [1975] proposed two ages for the

Stratoid Series (3.3 ± 0.1 and 3.3 ± 0.2 Ma) on a section where the lower Stratoid Series fails to outcrop. Furthermore, the eight closest dated samples (less than 30 km away from the Barberi site), dated in different studies, are all younger than 2.3 ± 0.2 Ma. We consider that the four previous Barberi results overestimate the ages. In the north-eastern part of the studied area, *Civetta et al.* [1974] proposed three ages which are in disagreement with about 20 analyses performed by three different laboratories. If one follows the geological map, they are located in the stratoid

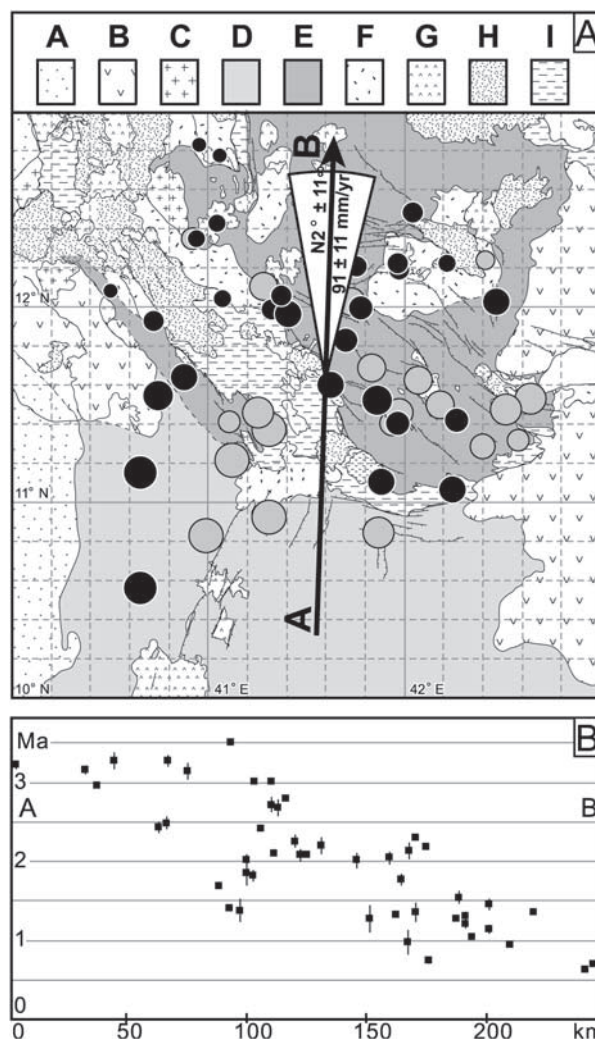


Figure 4. (a) Direction of migration of Stratoid Series emplacement. Ages are indicated by the circle size. Black circles: Cassagnol-Gillot technique [this work; *Audin*, 1999; *Kidane et al.*, 2002; *Manighetti et al.*, 1998] dating performed by PYG for the 1:100,000 Geological Map of the Republic of Djibouti. Gray circles: Ages by other techniques [*Zumbo et al.*, 1995, *Courtillot et al.*, 1984, *Gasse et al.*, 1980, *Richard*, 1979, *Civetta et al.*, 1974, *Barberi et al.*, 1972, 1974] (Ages performed by B.R.G.M. K/Ar laboratory). AB vector and angular sector: direction and rate of migration and 2σ confidence level obtained by fitting a plane to the data (see text). (b) Projection of data of Figure 4a along a $2^\circ N$ profile.

formation, but in an intensely faulted area they might actually not correspond to the stratoid unit. We therefore prefer to exclude these older results, which had been performed on whole rocks and where the authors themselves suspected some amount of radiogenic argon excess.

[30] Now, using this corrected database, we have extracted the oldest age determination in each 12' arc square, giving a constraint on the onset of the stratoid series formation in each part of the CAD. The 130 K-Ar ages available cover 46 space units and sample an area of 23000 km², about half of the Stratoid Series outcrop. Oldest samples selected range from 0.62 ± 0.01 to 3.5 ± 0.3 Ma (Figure 4a). The spatial distribution of these ages confirms the general south to north trend of migration of Stratoid Series volcanism, from about 3.5 Ma near stable Africa to about 1 Ma at 12°30'N. If we project these data along a north-south-trending profile (Figure 4b), the propagation of the stratoid volcanism onset becomes quite obvious, despite the complexities introduced by the southeastward propagating Manda Hararo-Manda Gargori rift and the northwestward propagating Ghoubbet Asal-Manda Inakir rifts.

[31] A quantitative estimate of the direction and speed of propagation can be made by fitting a plane surface to the data (Figure 4a). The fit is quite good, with a goodness-of-fit of 65% and a correlation coefficient of 0.81. With 43 degrees of freedom, the fit is highly significant (F test value of 39.9 versus a critical value of 3.3 [e.g. *Davis*, 1986]). At the 95% confidence level, the corresponding direction and velocity of northward drift of volcanic activity (perpendicular to that of rift propagation) are $2^\circ \pm 11^\circ\text{N}$ and 91 ± 11 mm/yr, respectively. Total migration of the center of Stratoid Series activity over the main 2.3- to 0.5-Ma period of this activity has therefore been on the order of 150 km. In the same time, rotation of the Danakil block with respect to Ethiopia [*Manighetti*, 1993; *Sichler*, 1980] has led to a total extension on the order of 30 km, whereas current rates of Arabia-Nubia motion predict a similar displacement [*Jestin and Huchon*, 1992]. The discrepancy between these figures underlines both the highly asymmetrical location of current rifting within the depression and the evolution from diffuse magmatism to concentrated rift activity. This is also consistent with the picture of early (pre-4 Ma) breakup in southern central Afar, when the Gulf of Aden propagator was blocked at the Shukra el Sheik discontinuity and penetrated into Afar through the Hol Hol strike-slip fault system [*Audin*, 1999; *Manighetti et al.*, 1998].

5.4. Transition Between the Stratoid Series and Presently Active Rift Segments

[32] Until the 1980s, the lack of precise ages prevented precise constraints on the evolution of presently active rift segments. Our many new age data on the youngest volcanic series (i.e. <1 Ma) of Afar allow a clearer picture. Active rift segments are actually located on both sides of the AD. *Manighetti et al.* [1998] suggested that these zones are localized where lithospheric necking occurred and that a lower volume of Stratoid Series magma was erupted there than in the center of the depression. A direct consequence of the lateral positions of the two propagating plate boundaries is that they do not connect yet and define an area where the onland continuations of the Red Sea and Gulf of Aden rift systems overlap [*Tapponnier et al.*, 1991]. Figure 5 shows a

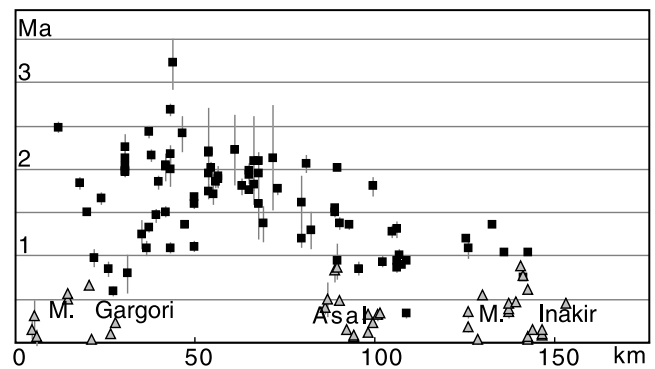


Figure 5. Projection of ages from the overlap zone along a profile oriented in the direction of plate motion. Black squares: Stratoid Series. Gray triangles: rift segments.

projection along a SW-NE section, from Dama Ale to Manda Inakir (corresponding to the Danakil-Somalia motion vector), of the 128 ages available in the overlap zone. This outlines the time-space history of emplacement of volcanic activity in central Afar. Between 3.5 and 1.5 Ma, from the earliest phases of Stratoid Series volcanism to the end of the first main volcanic crisis, magmatic activity was very diffuse, occupying a wide area of the Southern Depression up to 12°N. There are few data from 3.5 to 2.5 Ma, and a stepwise increase at about 2.3 Ma to a much more active (at least data-abundant) mode. After 1.5 Ma (or, strictly speaking, 1.75 Ma, taking into account the data with the smallest uncertainties), there are no Stratoid Series data points in a triangular area defined by the projection of the northeastern limit of the Manda Hararo-Manda Gargori rift segment and the Ghoubbet Asal segment (Figure 5). This sector corresponds exactly to the position of the overlap as defined by *Tapponnier et al.* [1991]: magmatic events became progressively localized on the edges of the overlap. Also, during this period, Stratoid Series volcanism migrated from the center of the CAD to its margins. Clusters of points corresponding to currently active rift segments (from 0.5 Ma to the present) follow two migration paths which define the gap. These rift segments can be considered as the last stage of the general volcano-tectonic evolution in Afar since 3.5 Ma, from diffuse activity over a large uniform area to multiple smaller and more concentrated rift segments in two narrow marginal zones. This volcanic evolution in time and space is particularly visible for the southwestern part of the overlap (Figure 5). In this case, attempting to separate lava associated with earlier Manda Hararo-Goba'ad volcanic activity from later Stratoid Series basalts is very hazardous. The NE migration trend seems slightly faster than the SW one. This is consistent with the main regional direction of migration of Afar volcanism as previously described.

6. Relationship Between Construction of Silicic Central Volcanoes and Propagation of Rift Segments

6.1. Regional Context of Eruption

[33] The proportions of evolved and basaltic volcanic products (bimodal Afar volcanism) are about 20 and 80%, respectively [*Barberi and Santacroce*, 1980]. These two compositional end-members differ in their styles of erup-

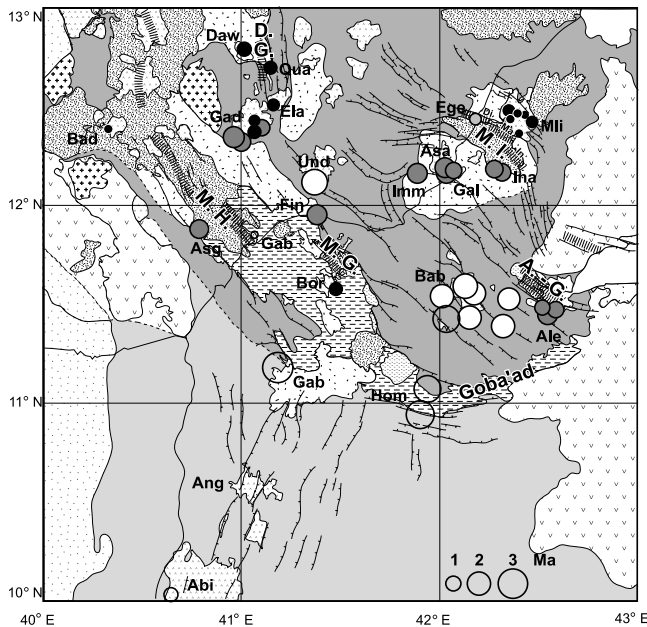


Figure 6. Location of silicic samples and central volcanoes. White, gray, black circles: first, second, and third main periods of silicic activity (area of circles as a function of age). Empty circles: others ages. Silicic centers: Abi, Abida-Ayalu; Ale, Asa Aleyta and Eger Aleyta; Ang, Angudi; Asa, Asa Ale; Asg, Asgura; Bab, Babba'Olou; Bad, Badi; Bor, Borawli; Daw, Dawa Ale; Ege, Egersuwa; Fin, Finini; Gal, Gabalti; Gab, Gablaytu; Gad, Gad'Elu; Hom, Homor; Imm, Immino; Ina, Inakir; Mli, Moussa Ali; Qua, Quarry.

tion. Fissural activity is the common mode for transitional basaltic lava flows, whereas evolved ones are more commonly found in the 20 or so “cumulo-volcanoes” erupted through or within the upper stratoid unit and Gulf Basalts and inside the presently active rift zones. Although important variations have been noted from one volcano to another, most of them do not seem to grow as a final stage of evolution of basaltic central volcanoes, contrary to what is observed in the Erta Ale range [Barberi and Varet, 1970; Treuil and Varet, 1973]. In contrast, these central silicic volcanoes were built up by successive outpouring of lavas, often as obsidians and sometimes as crystalline rhyolites [Barberi *et al.*, 1974]. Due to the low level of volatile phases, except in the northern Ethiopian rift, pyroclastites are scarce and summit calderas are rare. Prior to the present work, very few silicic central volcanoes had been dated. The 18 new ages available for these structures (Figure 6) support a heterogeneous distribution of silicic volcanism, with three main periods where it has been more important (double black arrows and lower black line in Figure 3b).

[34] Despite poor constraints on timing of emplacement, Undurur and Babba'Olou volcanoes seem to have been more or less contemporaneous, erupting about 2 Myr ago (Figure 6), which is contemporaneous with the first peak of Stratoid Series volcanism (Figure 3b). These volcanoes are presently located in central Afar, at equal distances from the Manda Hararo-Goba'ad system and Asal-Manda Inakir systems. The second period occurred from about 1.5 to 1.3 Ma, synchronous with the second volcanic peak, and

corresponds to eruption of the Finini volcano (near Serdo, NE of Manda Hararo) and the Asgura unit (near Loggia, SW of Manda Hararo). This period was quickly followed by another short one at about 1 Ma, when the first stage of Gad'Elu volcano, the margins of the Manda rift segment, and Eger Aleyta unit (S of Asal margin) were emplaced. Other volcanoes were active during these two periods, which may merge into a single one: the Asa Ale volcano, and more generally the acid volcanism of the Gawwah plateau (now also observed at the base of the Immino fault), and the Asa Aleyta unit (SE of Asal margin). In terms of silicic activity, the most productive period was from 0.65 to 0.25 Ma, when numerous central volcanoes erupted over a large area of the CAD: Borawli (Manda Gargori, north of Aisa Aita), Egersuwa (north of the Manda Inakir rift segment), Dawa Ale (west of Dadar Graben), Quarry (east of Dadar Graben), Ela (south of Dadar Graben), Badi (NW of Manda Hararo), the second stage of Gad'Elu, and the main silicic activity on Moussa Ali. This phase occurred just before the most recent peak in volcanic activity, which corresponds to the latest thrust of the Aden (Manda Inakir) and Red Sea (Manda Gargori) propagators.

[35] In the last 0.25 Myr, no significant silicic activity is observed in southern and central Afar, excepted for a few local volcanoes, such as Gablaitu on the Manda Hararo rift segment. However, Bidu, the largest silicic strato-volcano located in northern Afar (Figure 1), displays well-preserved flanks, suggesting important recent activity.

[36] The distribution in space of these silicic volcanoes is not random. The youngest ones are systematically located inside axial rift zones, while older ones are located at their external margins. Furthermore, silicic volcanoes in central Afar are younger when they are located closer to presently active extensive zones. We next highlight some systematic features regarding the space-time distributions of silicic volcanism and extensive zones in the main rift segments.

6.2. The Manda Hararo-Goba'ad System

[37] The Manda Hararo-Goba'ad system corresponds with the recent SE termination of the Red Sea propagator into central Afar [Manighetti *et al.*, 1998] (Figures 1a and 1b). The northernmost rift segment in this system is characterized by a large volume of silicic lava. Unfortunately no age data are available there. However, it is characterized by the presence of internal volcanoes affected by the youngest rift faults and by more weathered and dismantled marginal volcanoes. The central rift segment, the Manda Hararo *sensu stricto*, is the most accessible and best constrained timewise. It is largely covered by the lower Awash plain lacustrine deposits, except for two lateral zones and a central one, 15 and 30 km wide, respectively, where basaltic lavas still outcrop. On both margins of the central Manda Hararo (CMH), two silicic centers outcrop, the Finini volcano (75BY1, 1.32 ± 0.015 Ma) to the NE and the Asgura volcano (75AL, 1.27 ± 0.17 Ma) to the SW. The ages of the basaltic lavas, which form the external margin of CMH and correspond to the beginning of the initiation of the future active rift, range from 1.1 ± 0.1 to 0.6 ± 0.1 Myr [this study; Kidane *et al.*, 2002]. They are also systematically younger than the acidic lavas. The same schema is observed for the younger axial fissure-fed basaltic lava flows. Ages available on them range from 0.22 ± 0.05 Ma

to present, and they are all younger than the silicic Badi volcano (80AE3, ~ 0.29 Ma).

[38] The later stage of propagation of the Manda Hararo-Goba'ad system has led to the emplacement of the Manda Gargori, the youngest and less-developed rift segment. It is located north of the town of Aisa Aita, and it is three times narrower than the Manda Hararo rift segment, in agreement with increased concentration of volcanism with time [Manighetti *et al.*, 1998]. Fissure-derived basaltic lavas are affected by N150°-oriented faults with small vertical throws due to the youth of the extensive structure. Older eruptive units display ages as old as 0.22 ± 0.02 Ma, while younger ones are historical. Manda Gargori is located between a 0.556 ± 0.007 Ma silicic central volcano (Borawli) to the southwest and the external limit of CMH to the northeast (Figures 1b and 6). The latter is characterized by the presence of several silicic eruptions which do not form a central edifice but rather outcrop sporadically over an older basaltic lava field dated at 0.66 ± 0.10 Ma (Table 1). No ages are available for the silicic outcrops, but they must both be considered younger than the basaltic plateau and older than the faults which cut across them, i.e., between 0.66 ± 0.10 and 0.22 ± 0.02 Ma. Therefore, as also observed for the Manda Hararo, the Manda Gargori rift segment is located between two silicic centers which erupted before the beginning of rift emplacement.

6.3. The Manda Inakir Rift Zone

[39] Space-time coherency of silicic activity is also observed in the Manda Inakir (hereafter MI, Figure 6) rift segment, which is connected to the Asal rift segment by the Makarassou transfer fault system [Tapponnier and Varet, 1974]. This 50×20 km² large extensional structure comprises two shield volcanoes, the Manda and the Inakir, formed through fissural magmatism [De Fino *et al.*, 1973], with lava erupted from 0.87 ± 0.15 Ma [Manighetti *et al.*, 1998] onward. Rift zones, located on the northern side of the shield volcanoes, can be subdivided into three rift segments (Inakir, Manda, and Dirko Koma, Figure 2), which correspond to three different stages of propagation of the plate boundary from ESE to WNW, since about 0.2 Ma [Manighetti *et al.*, 1998]. Axial lavas affected by the Manda rifting range from 0.14 ± 0.02 Ma to the present [Lahitte, 2000; Manighetti *et al.*, 1998]. Few central volcanoes still outcrop at the periphery of the shield volcanoes. To the south of the Inakir segment, an evolved lava flow sequence displays two ages at about 1.05 ± 0.03 Ma, older than the oldest basaltic flow of the Inakir volcano. To the north of the Inakir shield volcano, some large silicic domes are situated along the trend extending from the youngest rift segment. We have sampled the largest one, the Egersuwa, which represents about 2 km³ of erupted lava (Figures 1b, 6 and 7). It is actually partly dismantled by the faults associated with the Dirko Koma rift segment, which is the most advanced tip of the Aden propagator. All volcanic activity on these domes is silicic (ranging from 0.44 ± 0.01 to 0.35 ± 0.01 Ma), except for the last lava flows, which are basaltic (0.35 ± 0.01 Ma, Table 1 and Figure 7).

[40] At a larger scale, on both external margins of the MI rift zone, larger silicic volcanoes are present. To the northeast, the Moussa Ali volcano represents more than 50 km³ in volume. Ages range from 0.73 ± 0.01 to 0.17 ± 0.02 Ma.

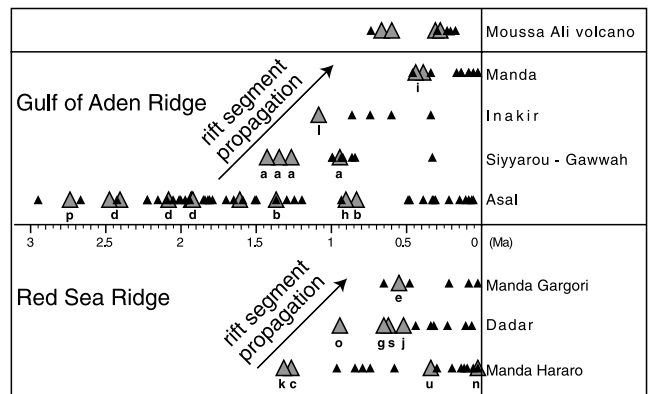


Figure 7. Relation between silicic activity and initiation and propagation of rifting. Silicic (large gray triangles) and basaltic (small black triangles) volcanic activity as a function of time for the main rift segments associated to the propagation of the Red Sea and Gulf of Aden Ridges. Letters: silicic activity as in Figure 1b (except u, Badi volcano), locations in Figures 1b and 6.

These values probably do not represent the overall activity, which must have started about 1 Ma. Three main phases of activity are defined: before 0.6 Ma, from 0.35 to 0.25 Ma, and after 0.25 Ma. The first two are the most important and mainly emitted evolved products (our sampling underestimates this proportion, Figure 7). The earliest basaltic lava flows erupted at the axis of the Manda rift segment immediately succeeded the latest ones associated with the third stage of the Moussa Ali volcano, which is totally basaltic. These two styles of volcanism have almost the same geochemical composition [Lahitte, 2000]. As clearly shown by Figure 7, volcanic activity alternated between the Moussa Ali volcano and MI rift segment. Further silicic volcanism occurred prior to initiation of the fissural volcanism of the MI rift segment at 0.14 ± 0.02 Ma on the Moussa Ali as well on Egersuwa.

[41] In the same fashion, to the south, just beyond the basaltic fissural lavas erupted by the Manda volcano, some smaller silicic centers cluster and occupy most of the surface of the Gawwah plateau, where about 30 km³ of silicic lavas were erupted, during two main stages (Figures 1b and 6). The first stage is totally silicic and occurred between 1.35 ± 0.02 and 1.33 ± 0.04 Ma (but it is reasonable to consider that activity was longer). It corresponds to the eruption of the 200-m-high Asa Ale volcano, located south of Gawwah plateau, the last activity of which corresponds to pyroclastic episodes and caldera emplacement. After that, no activity seems to occur before the beginning of the second stage, about 0.95 ± 0.02 Myr ago, which is characterized by the eruption of a few small silicic domes. They were directly overlain by the emplacement of the 200-m-thick Gulf Basalts sequence, until 0.85 ± 0.02 Ma. Some later phases occurred at 0.33 ± 0.01 Ma, just before MI initiation.

[42] In the three cases of Gawwah plateau, the Moussa Ali volcano, and the Egersuwa, respectively at the southwestern, northeastern, and northern edges of the MI rift segment, volcanism began by a polyphase silicic activity, followed by fissural basaltic activity. We observe that the beginning of MI rift segment activity [~ 0.2 kyr; Manighetti

et al., 1998] is coeval with the first basaltic activity on Manda Gargori (0.22 ± 0.02 Ma, this work). These two rift segments, which were activated at approximately the same time, mediated both the propagation of Aden rifting to the NW and of Red Sea rifting to the SE, maintaining the width of the overlap roughly constant, as suggested by *Tapponnier et al.* [1991] and fully elaborated on by *Manighetti et al.* [2001].

6.4. The Asal Rift

[43] Our study does not provide new results within the Republic of Djibouti or on the Asal rift. However, previous studies [*Barberi et al.*, 1974; *Courtilot et al.*, 1984; *Zumbo et al.*, 1995] reported about 10 ages on evolved rock samples between 100 and 10 km away from the presently active rift zone. On the external margins of the Asal-Ghoubbet (AG) rift segments, few silicic centers outcrop. Two of them have been dated: Asa Aleyta and Eger Aleyta. Ages from the main phase of eruption range from 1.4 ± 0.3 to 0.76 ± 0.08 Ma [*Mazet and Recroix*, 1986; *Zumbo et al.*, 1995], with a pulse of volcanism occurring around 0.95 ± 0.10 Ma. Acid phases preceded the emplacement of the presently active rift segment, which started propagating about 0.8 Ma [*Manighetti*, 1993]. South of Asal, silicic volcanism outcrops sporadically from Eger Alayta to the northern margin of the Goba'ad graben, with ages ranging from 1.6 ± 0.1 to 2.75 ± 0.06 Ma and increasing rather regularly with distance away from the AG rift (Figures 6 and 7). The more important silicic central volcano of Babba'Olou can be associated within this trend. It is located 50 km WSW of the Asal rift and displays ages ranging from 2.4 to 1.9 Ma, with a main phase around 2 Ma. Some rhyolitic and trachytic lavas outcrop on the margins of the Hanle and Gaggade grabens and can be considered as lateral projections from this volcano before it was dismantled by the extensive fault system that propagated in central Afar.

[44] We should note some interesting similarities in the relationship between the major silicic volcanoes and the rift zones within the CAD. For the Asal-Ghoubbet, MI, and Manda Hararo rift segments, a large silicic volcano erupted nearby (a few 10 km), approximately 1 Myr before the rift segment was initiated; these are, respectively, the Babba'Olou, Gawwah, and Undurur volcanoes.

6.5. Other Extensional Zones

[45] Because of subsequent volcano-tectonic activity, the first trace of rift propagation is often hidden in the Asal Ghoubbet-MI and Manda Hararo-Manda Gargori rift zones (Figure 1b). Fortunately, two other extensional structures, the Dadar graben and the much larger Ethiopian rift, either aborted or remained in an incipient stage [*Courtilot et al.*, 1987], displaying features typical of the preliminary phases of rift propagation of the Red Sea and Aden ridges (Figures 1a and 1b).

[46] The Dadar Graben is aligned with the Erta Ale and Tat'Ali strato-volcanoes and is affected by a system of normal faults striking approximately 165° but is presently inactive despite evidence for important extensional activity [*Lahitte et al.*, 2001]. On each margin, rhyolitic volcanism is present: Dawa Ale (0.62 ± 0.01 Ma) and Quarry dome (0.65 ± 0.01 Ma), to the west and east, respectively. Prior to rift propagation, these two edifices would have formed a

single structure which is now dismantled and cut by the axial depression. Farther to the south, the Ela volcano (0.52 ± 0.01 Ma), whose activity is mainly silicic but which ends with basaltic activity, has also been dismantled by the normal faults. All ages determined on fissure-derived basaltic lavas which erupted in the Dadar Graben between Dawa Ale and Quarry volcanoes range between 0.07 ± 0.05 and 0.46 ± 0.18 Ma, and are younger than acidic lavas from this area. Though it is apparently not an active part of the Red Sea propagator today, the Dadar Graben displays the same organization, with some older marginal silicic centers erupted prior to the main fissural basaltic phase.

[47] Due to its low rate of extension (4 mm/yr [e.g., *Jestin and Huchon*, 1992]), the Ethiopian rift displays a low magmatic flux and offers another good context to study the link between the silicic activity and rift activity. Three important volcanoes (from south to north Abida-Ayalu, Angudi, and Gabilema), about 50 km apart and aligned with the topographic axis of the Addabo graben, are located along its northernmost 100 km (Figures 1a and 6). Unfortunately, they are still poorly documented and without chronological constraints. However, the Geological Map of Afar and Spot image analyses show that their earlier (intermediate to evolved) lavas overlap the upper Stratoid Series. These volcanic products are now strongly affected by $N20^\circ$ normal faults but still outcrop on the margins of the graben. The subsequent, more basic products of these three volcanoes seal some of the faults and acid lavas. No Holocene volcanism occurs along the graben, showing that activity there is limited to the strato-volcanoes.

7. Conclusions

[48] Because of a lack of sufficiently precise K-Ar ages, the evolved eruptive centers of Afar had not previously been understood in the context of Red Sea and Aden ridge propagation. We have now obtained strong temporal constraints, which allow us to describe the interaction between silicic activity and rift propagation. We provide evidence that such an association is the rule rather than the exception. We interpret these as events which occurred systematically during continental rift propagation within central Afar of the Red Sea and Gulf of Aden Ridges. Both at the larger scale of a whole rift and at the smaller scale of a rift segment, propagation and migration of the ridge are preceded by the eruption of significant volumes of silicic magmas which form central volcanoes on the edges of the future rift segment. Furthermore, each stage of concentration of volcano-tectonic activity inside a rift zone is also preceded by the eruption of silicic lavas.

[49] The evolution of volcanism can be linked to the degree of extension which mediates ridge propagation. With lower levels of extension, direct eruption of magma to the surface is more difficult, and magmatic chambers are formed. Silicic volcanism corresponds mainly to the ultimate stage of a differentiation process which evolved quickly from basaltic magma to trachy-rhyolite compositions [*Barberi et al.*, 1980; see also *Lahitte*, 2000; *Treuil and Varet*, 1973]. Therefore, evolved products were located at the top of these reservoirs and were erupted first when extensional rates increased, during the earlier phases of rift segment emplacement. This mechanism can also justify the

bimodal volcanism of Afar. During stages with low levels of fracturing, magmas were more or less stocked in intermediate reservoirs which allowed them to evolve from primitive basalts to rhyolites. With increasing extension, faults and fissures presented the magma with new and easier paths to the surface. Silicic lavas, which were located at the top of the magmatic chamber, were erupted first. Then, with faulting and fissuring becoming more and more intense, magmas were not stalled any more but were directly erupted from the source to the surface. This also explains why the latest volcanic activity on the few central volcanoes is often basaltic, with the same composition as the fissure-derived lavas of the newly created rift segment. Thus, the degrees of alkalinity of the different rift segments are in agreement with this model: they are greater at the tip of the propagator and lower on the more mature ridge [Deniel *et al.*, 1994; Treuil and Varet, 1973].

[50] Studies of local rift segments have shown that there exists a relation between faults, which propagate the ridges inside Afar, and the presence of central volcanoes, the former being generally younger than and cross-cutting and dismantling the latter. Due to the heat injected from the magmatic chambers of these volcanoes, the thickness of the cold continental crust is lower. During increased extension, they could form zones of local weakness which would concentrate stress and capture nearby faults. This phenomenon has been previously observed and described by Van Wyk de Vries and Merle [1996] for the Fieaele volcano on the Asal rift segment. We therefore suggest that the zones near central volcanoes have the same influence, at the local scale of a rift segment, as at the marginal zones of the AD, where stress is concentrated because of thinner weakened continental crust at the regional scale of a ridge propagator [Manighetti, 1993]. In this respect, silicic central volcanoes would play the same role with respect to local rift segment propagation as a mantle plume and flood basalts with respect to continental breakup at the largest scale, as proposed by Courtillot *et al.* [1999]. In both cases, emplacement of extensional structures would be promoted by two effects: on the one hand, an “active” magmatic component (central volcanoes for Afar rift segments, mantle plumes for midoceanic ridges, actually intervening to alter crustal and lithospheric rheology); and on the other hand, a passive tectonic component (the local extensional stress field for Afar rift segments, the large-scale plate boundary forces linked with the geodynamical context for the Aden and Red Sea midocean ridges and the Ethiopian continental rift).

[51] Based on those K-Ar ages which represent the most recent phases of activity on central silicic volcanoes, we can infer the likely emplacement of future rift segments. The Bidu volcano is an important silicic volcanic complex, located to the NW of the MI rift segment (Figure 1a). Manighetti *et al.* [1998] have suggested that the ultimate connection of the Aden ridge with the Red Sea rift will be established near Bidu. This volcano is indeed approximately aligned with the youngest fractures associated with Aden Ridge propagation (i.e., the MI and Northern Makarassou transfer fault). Considering the mechanism outlined above, this volcanic complex could capture these most advanced fractures of the Aden Ridge. After migrating northward in southern Afar (between Asal and MI), the tear zone could veer and follow a NW direction, which would maintain it

near the eastern margin of the Afar zone of weakness, avoiding cutting across the thicker and colder crust of the Danakil horst. The southern tip of the undersea part of the Red Sea Ridge is located only a few tens of kilometers north of the Bidu volcano, and could connect with the Aden ridge. This connection would progressively bypass the emerged rift segments of the Red Sea Ridge (Erta Ale, Alayta, Manda Hararo-Goba'Ad) in favor of the emerged rift segments of the Aden ridge (Asal, MI; Figure 1a). Our interpretation of K-Ar ages and compositional data thus converges with the tectonic interpretation of Manighetti *et al.* [1998], and the two provide independent support for this rather simple multiple-scale tectonic and geodynamical scenario.

[52] **Acknowledgments.** This work took place as part of a collaboration program that was established between INSU-CNRS in France and the Department of Geology and Geophysics of the University of Addis-Abeba in Ethiopia. We thank the French Center of Ethiopian Studies that greatly facilitated field logistics. The manuscript was greatly improved thanks to suggestions from D. L. Pinti and X. Quidelleur. R. Duncan and an anonymous reviewer are thanked for their useful comments. This work has been supported by the region Ile de France grant SESAME 947. This is LGMT contribution 32 and IGP contribution 1830.

References

- Arthaud, F., P. Choukroune, and B. Robineau, Evolution structurale du golfe de Tadjoura et du Sud de la dépression Afar (République de Djibouti), *Bull. Soc. Geol. France*, 22, 909–915, 1980.
- Audin, L., Pénétration de la dorsale d'Aden dans la dépression Afar entre 20 et 4 Ma, Ph.D. thesis Univ. Paris 7 & IGP, Paris, 1999.
- Barberi, F., and R. Santacroce, The Afar Stratoid Series and the magmatic evolution of East African rift system, in *Colloque Rift d'Asal: Reunion Extraordinaire de la Société Géologique de France*, edited by Anonymous, pp. 891–897, Société Géologique de France, Paris, France, 1999.
- Barberi, F., and J. Varet, The Erta Ale volcanic range (Danakil depression, Northern Afar, Ethiopia), *Bull. Volc.*, 36, 917–948, 1970.
- Barberi, F., and J. Varet, Volcanism of Afar: Small-scale plate tectonics implications, *Geo. Soc. Am. Bull.*, 88, 1251–1266, 1977.
- Barberi, F., S. Borsi, G. Ferrara, G. Marinelli, R. Santacroce, H. Tazieff, and J. Varet, Evolution of the Danakil depression (Afar, Ethiopia) in light of radiometric age determinations, *J. Geol.*, 80(6), 720–729, 1972.
- Barberi, F., R. Santacroce, and J. Varet, Silicic peralkaline volcanic rocks of the Afar depression (Ethiopia), *Bull. Volc.*, 38, 755–790, 1974.
- Barberi, F., R. Ferrara, R. Santacroce, and J. Varet, Structural evolution of the Afar triple junction, in *Afar depression of Ethiopia*, edited by A. Pilger and A. Roesler, pp. 39–53, Schweizerbart, Stuttgart, Germany, 1975.
- Barberi, F., R. Santacroce, and J. Varet, Chemical aspects of rift magmatism, in *Final Report of the International Geodynamic Project on Continental and Oceanic Rifts*, edited by P. A. Sigvaldason, 1980.
- Black, R., W. H. Morton, and D. C. Rex, Block tilting and volcanism within the Afar in the light of recent K/Ar age data, in *Afar Depression of Ethiopia*, vol. 1, edited by A. Pilger and A. Roesler, pp. 296–300, Schweizerbart, Stuttgart, Germany, 1975.
- Cassignol, C., and P.-Y. Gillot, *Range and Effectiveness of Unspiked Potassium-Argon Dating: Experimental Groundwork and Applications*, pp. 159–179, John Wiley, New York, 1982.
- Chessex, R., M. Delaloye, J. Muller, and M. Weidmann, Evolution of the volcanic region of Ali Sabieh (T. F. A. I.), in the light of K-Ar age determinations, in *Afar Depression of Ethiopia*, vol. 1, edited by A. Pilger and A. Roesler, pp. 221–227, Schweizerbart, Stuttgart, Germany, 1975.
- Choukroune, P., B. Auvray, and B. Francheteau, Tectonics of the westernmost Gulf of Aden and the Gulf of Tadjoura from submersible observations, *Nature*, 319, 396–399, 1986.
- Choukroune, P., B. Francheteau, B. Auvray, J.-M. Auzende, J. P. Brun, B. Sichler, F. Arthaud, and J. C. Lépine, Tectonics of an incipient oceanic rift, *Mar. Geophys. Res.*, 9, 147–163, 1988.
- Civetta, L., M. De Fino, P. Gasparini, M. R. Ghiara, L. La Volpe, and L. Lirer, Structural meaning of east-central Afar volcanism (Ethiopia T. F. A. I.), *J. Geol.*, 83, 363–373, 1974.
- Coulié, E., X. Quidelleur, P.-Y. Gillot, J.-C. Lefèvre, and S. Chiesa, Combined ⁴⁰Ar/³⁹Ar and K/Ar dating of Ethiopian and Yemenite traps volcanism, *Eos Trans. AGU*, 81(48), Fall Meet. Suppl., abstract V21D-22, 2000.
- Courtillot, V., A. Galdéano, and J. Le Mouél, Propagation of an accreting plate boundary: A discussion of new aeromagnetic data in the Gulf of Tadjoura and southern Afar, *Earth. Planet. Sci. Lett.*, 47, 144–160, 1980.

- Courtilot, V., J. Achache, F. Landre, N. Bonhommet, P.-Y. Galibert, R. Montigny, and G. Féraud, Episodic spreading and rift propagation: New paleomagnetic and geochronologic data from the Afar passive margin, *J. Geophys. Res.*, **89**, 3315–3333, 1984.
- Courtilot, V., R. Armijo, and P. Tapponnier, Kinematics of the Sinai triple junction and a two phase model of Arabia-Africa rifting, in *Continental Extensional Tectonics*, edited by M. P. Coward, J. F. Dewey, and P. L. Hancock, pp. 559–573, Blackwell Sci., Malden, Mass., 1987.
- Courtilot, V., C. Jaupart, I. Manighetti, P. Tapponnier, and J. Besse, On causal links between flood basalts and continental breakup, *Earth Planet. Sci. Lett.*, **166**, 177–199, 1999.
- Cox, K. G., J. D. Bell, and R. J. Pankurst, *The Interpretation of Igneous Rocks*, p. 450, Allen and Unwin, Concord, Mass. [c/o Paul & Co.], 1979.
- Dagain, J., M. Fournier, and F. Gasse, *Geological Map of Djibouti*, scale 1:10,000, map and notice of Dikhil sheet, ISERST, Paris, 1985.
- Davis, J. C., *Statistical and Data Analysis in Geology*, p. 646, John Wiley, New York, 1986.
- De Fino, M., L. La Volpe, L. Lierer, and J. Varet, Geology and petrology of Manda-Inakir range and Moussa-Ali volcano, central eastern Afar (Ethiopia and T. F. A. I.), *Rev. Geogr. Phys. Geol. Dyn.*, **15**(4), 373–386, 1973.
- Deniel, C., P. Vidal, C. Coulon, P.-J. Vellutini, and P. Piguet, Temporal evolution of mantle sources during continental rifting: The volcanism of Djibouti (Afar), *J. Geophys. Res.*, **99**(B2), 2853–2870, 1994.
- Fournier, M., and O. Richard, *Geological Map of Djibouti*, scale 1:10,000, map and notice of Loyada sheet, ISERST, Paris, 1984.
- Fournier, M., F. Gasse, J. C. Lepine, O. Richard, and J. C. Ruegg, *Geological Map of Djibouti*, scale 1:100,000, map and notice of Djibouti sheet, ISERST, Paris, 1983.
- Fournier, M., F. Gasse, J. C. Lepine, O. Richard, and J. C. Ruegg, *Geological Map of Djibouti*, scale 1:100,000, map and notice of Tadjoura sheet, ISERST, Paris, 1984.
- Gass, I. G., Tectonic and magmatic evolution of the Afro-Arabian dome, in *African Magmatism and Tectonics*, edited by T. N. Clifford and I. G. Gass, pp. 285–300, Hafner, Old Tappan, N. J., (imprint of Macmillan), 1970.
- Gasse, F., O. Richard, P. Robbe, P. Rognon, and M. Williams, Evolution tectonique et climatique de l'Afar Central d'après les sédiments plio-pléistocènes, *Bull. Soc. Géol. Fr.*, **22**(7), 987–1001, 1980.
- Gillot, P.-Y., and Y. Cornette, The Cassinon technique for potassium-argon dating, precision and accuracy: Examples from the late Pleistocene to recent volcanics from southern Italy, *Chem. Geol.*, **59**, 205–222, 1986.
- Gillot, P.-Y., Y. Cornette, N. Max, and B. Floris, Two reference materials, trachytes MDO-G and ISH-G, for argon dating (K-Ar and 40Ar/39Ar) of Pleistocene and Holocene rocks, *Geostandards Newsl.*, **16**(1), 55–60, 1992.
- Guérin, G., and G. Valladas, Thermoluminescence dating of plagioclase, *Nature*, **206**, 697–699, 1980.
- Hofmann, C., V. Courtilot, G. Ferauc, P. Rochette, G. Yirgus, E. Ketefo, and R. Pik, Timing of the Ethiopian flood basalt event and implications for plume birth and global change, *Nature*, **389**, 838–841, 1997.
- Irvine, T. N., and W. R. A. Baragar, A guide to the chemical classification of the common volcanic rocks, *Can. J. Earth Sci.*, **8**, 523–548, 1971.
- Jestin, F., and P. Huchon, Cinématique et déformation de la jonction triple Mer Rouge-Golfe d'Aden-Rift Ethiopien depuis l'Oligocène, *Bull. Soc. Géol. Fr.*, **163**(8), 125–133, 1992.
- Kidane, T., Contribution à l'étude paléomagnétique et géochronologique de l'évolution cinématique de la dépression Afar au cours des trois derniers millions d'années, Ph.D. thesis, Univ. Paris 7 & IPGP, Paris, 1999.
- Kidane, T., V. Courtilot, I. Manighetti, L. Audin, P. Lahitte, X. Quidelleur, P.-Y. Gillot, Y. Gallet, J. Carlut, and T. Haile, New paleomagnetic and geochronologic results from Ethiopian Afar: Block rotations linked to rift overlap and propagation, and determination of a 2 Ma reference pole for stable Africa, *J. Geophys. Res.*, **108**, doi:10.1029/2001JB000645, in press, 2002.
- King, S. D., and D. L. Anderson, An alternative mechanism of flood basalt formation, *Earth Planet. Sci. Lett.*, **136**, 269–279, 1995.
- Lahitte, P., Le volcanisme plio-quaternaire lié aux mécanismes d'ouverture de la dépression Afar, Ph.D. thesis, Univ. Paris-Sud, Paris, 2000.
- Lahitte, P., E. Coulié, N. Mercier, T. Kidane, and P.-Y. Gillot, Chronologie K-Ar et TL du volcanisme aux extrémités sud du propagateur Mer Rouge en Afar depuis 300 ka, *C. R. Acad. Sci. Paris*, **322**(1), 13–20, 2001.
- Manighetti, I., Dynamique des systèmes extensif en Afar, Ph.D. thesis, Univ. Paris 7 & IPGP, Paris, 1993.
- Manighetti, I., P. Tapponnier, P.-Y. Gillot, E. Jacques, V. Courtilot, R. Armijo, J. C. Ruegg, and G. King, Propagation of rifting along the Arabia Somalia plate boundary: into Afar, *J. Geophys. Res.*, **103**, 4347–4974, 1998.
- Manighetti, I., P. Tapponnier, V. Courtilot, Y. Gallet, E. Jacques, and P.-Y. Gillot, Strain transfer between disconnected, propagating rifts in Afar, *J. Geophys. Res.*, **106**, 13,614–13,665, 2001.
- Mazet, A. G., and F. Recroix, *Geological Map of Djibouti*, scale 1:100,000, map and notice of Ali Sabieh sheet, ISERST, Paris, 1986.
- Odin, G. S., *Numerical Dating in Stratigraphy*, p. 1094, John Wiley, New York, 1982.
- Richard, O., Etude de la transition dorsale océanique-rift émergé: Le golfe de Tadjoura (République de Djibouti), Ph.D. thesis, Univ. Paris-Sud, Paris, 1979.
- Richard, O., F. Gasse, M. Fournier, and J. C. Ruegg, *Geological Map of Djibouti*, scale 1:100,000, map and notice of Tadjoura sheet, ISERST, Paris, 1985.
- Schilling, J. G., Afar mantle plume: Rare earth evidence, *Nature*, **242**, 2–5, 1973.
- Sichler, B., La biette Danakile: Un modèle pour l'évolution géodynamique de l'Afar, *Bull. Soc. Geol. Fr.*, **22**, 925–933, 1980.
- Steiger, R. H., and E. Jäger, Subcommission on geochronology: Convention on the use of decay constants in geo and cosmochronology, *Earth Planet. Sci. Lett.*, **36**, 359–362, 1977.
- Tapponnier, P., and J. Varet, La zone de Mak'arrassou en Afar: Un équivalent émergé des failles transformantes océaniques, *C. R. Acad. Sci. Paris*, **278**, 209–212, 1974.
- Tapponnier, P., R. Armijo, I. Manighetti, and V. Courtilot, Bookshelf faulting and horizontal block rotation between overlapping rifts in southern Afar, *Geophys. Res. Lett.*, **17**, 1–4, 1991.
- Treuil, M., and J. Varet, Critères pétrologiques géochimiques et structuraux de la genèse et de la différenciation des magmas basaltiques: Exemple de l'Afar, Ph.D. thesis, Univ. Paris-Sud & Orléans, Paris, 1973.
- Valladas, G., P.-Y. Gillot, and G. Guérin, Dating plagioclase?, in *Specialist Seminar on TL Dating*, pp. 141–150, PACT Council Europe, Oxford, England, 1978.
- Van Wyk de Vries, B., and O. Merle, The effect of the volcanic constructs on the rift fault patterns, *Geology*, 643–646, 1996.
- Varet, J., Geological map of Afar, Cent. Natl. de la Rech. Sci. (CNRS), Paris, 1975.
- Varet, J., and F. Gasse, *Géologie de l'Afar Central et Méridional*, Cent. Natl. de la Rech. Sci. (CNRS), Paris, 1978.
- White, R. S., and D. P. McKenzie, Magmatism at rift zones: The generation of volcanic continental margins and flood basalts, *J. Geophys. Res.*, **94**(B6), 7685–7729, 1989.
- Wintle, A., Anomalous fading of thermoluminescence in mineral samples, *Nature*, **245**, 143–144, 1973.
- Zumbo, V., G. Féraud, P. Vellutini, P. Piguet, and J. Vincent, First 40Ar/39Ar dating on early Pliocene to Plio-Pleistocene magmatic events of the Afar-Republic of Djibouti, *J. Volcanol. Geotherm. Res.*, **65**, 281–295, 1995.

A. Bekele and T. Kidane, Department of Geology and Geophysics, University of Addis-Ababa, Ethiopia. (dgg@telecom.net.et)

V. Courtilot, Laboratoires de Paléomagnétisme et de Tectonique, Institut de Physique du Globe de Paris, 75230 Paris Cedex 05, France. (dgg@telecom.net.et; courtil@ipgp.jussieu.fr)

P.-Y. Gillot and P. Lahitte, Laboratoire de Géochronologie Multi-Techniques UPS-IPGP, Bat. 504, Sciences de la Terre, Université Paris-Sud, 91405 Orsay, France. (lahitte@geol.u-psud.fr; gillot@geol.u-psud.fr)